Column

▶Kaposi 肉腫以外の HHV-8 関連疾患

primary effusion lymphoma

primary effusion lymphoma（PEL：原発性体腔液性リンパ腫）は，胸水や腹水などの体腔液中に浮遊する形で増殖する B 細胞性の液性リンパ腫であり，通常，腫瘍塊を形成しない（Said ら，2008[1]；Nador ら，1996[2]）．HHV-8 の検出が PEL の診断には必須である．EBV も陽性である症例が多い．胸膜などの隣接する部位に固形腫瘍を形成することがある．また，まれに液性リンパ腫の形をとらず，皮膚，消化管などに HHV-8 関連固形リンパ腫として現れることがあり，これは extracavity PEL（体腔外 PEL）と呼ばれている．

若年から成年の HIV 陽性男性同性愛者に発症する例がほとんどで，約半数には Kaposi 肉腫の合併がみられる．まれながら移植後のレシピエント，高齢者での発症がある．胸腔，腹腔，心嚢腔が好発部位であり，こうした体腔液中に滲出液（胸水，腹水，心嚢水）が貯留する．リンパ節腫脹を伴わないのが普通である．AIDS 合併例では Kaposi 肉腫の既往がある症例が多い．通常，白血化はない．血中の IL-6 量が増加するが，ウイルスがコードする viral IL-6（vIL-6）の量も増加する．確立した治療法はなく，予後も悪い．extracavity PEL の発症部位は皮膚，消化管，肺などで，皮膚では皮下腫瘤として発症する．

病理所見

リンパ腫細胞のスメアやサイトスピン標本の Giemsa 染色では，リンパ腫細胞は大型の immunoblastic または plasmablastic な細胞から，anaplastic large cell 様の形態をとり，多彩である（1）．核は多形性に富み，明確な核小体が特徴的で，細胞質は比較的広く，好塩基性であり，plasma cell にみられる核周明庭を思わせる所見もみる．免疫染色では CD45（LCA）は陽性であるが，CD20，CD79a などの B 細胞マーカーはすべて脱落している．CD30，CD138 が陽性になることが多

1 PEL 症例のスメア標本

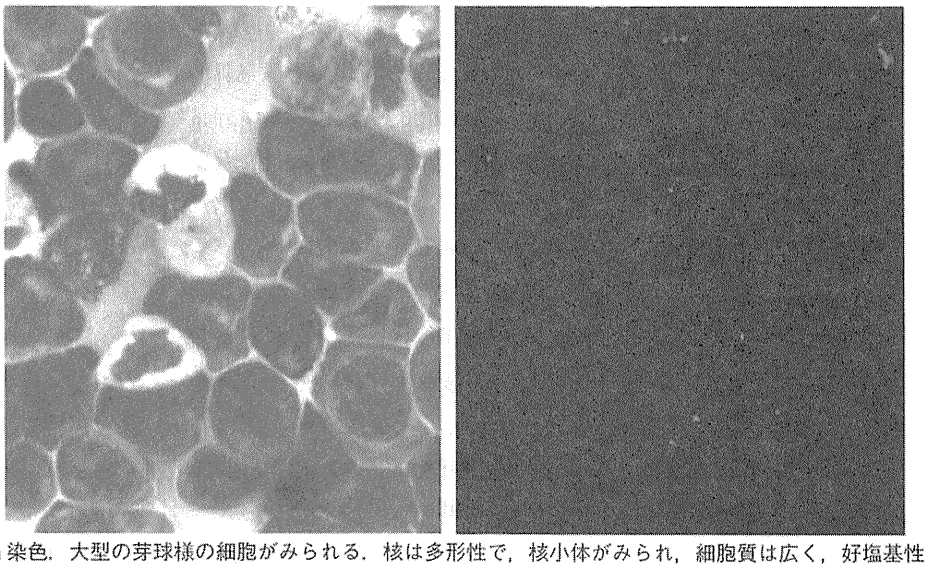

左：Giemsa 染色．大型の芽球様の細胞がみられる．核は多形性で，核小体がみられ，細胞質は広く，好塩基性に濃染する．核周明庭もみられ，plasma cell との類似を思わせる．
右：LANA-1 の蛍光免疫染色．ほとんどすべての細胞の核内に点状の陽性シグナルを認める．

い．HHV-8 の潜伏感染蛋白である LANA-1 がリンパ腫細胞には必ず陽性であり，これが唯一の PEL のマーカーといえる．

多巣性 Castleman 病

(multicentric Castleman disease：MCD)

Castleman 病は単発のリンパ節の過形成を主体とする疾患であり，Castleman 病が全身のリンパ節に多発した病変が MCD である．日本で長らく IPL(idiopathic plasmacytic lymphoadenopathy with polyclonal hyperimmunoglobulinemia) といわれていた疾患は MCD と同義と考えてよい．

全身のリンパ節腫脹に加え，多クローン性高ガンマグロブリン血症，発熱，貧血，白血球減少など多彩な症状を呈する．血清中の IL-6 および VEGF（血管内皮増殖因子）の上昇がみられる．組織学的にはリンパ節内の濾胞内に onion skin appearance と呼ばれる胚中心から同心円状に層をなす特徴的な硝子様物質と血管増生を伴うリンパ濾胞過形成を主体とする hyaline-vascular type（HV 型）と濾胞間組織に形質細胞の増加が目立つ plasma cell type（PC 型）がある（2）．MCD では PC 型が多いとされるが，実際には MCD でも両方の組織型が混在していることが多い．

単発の Castleman 病は切除し完治するが MCD は予後不良である．すべての症例で HHV-8 が検出されるわけではなく，むしろ，日本人症例では HHV-8 陽性 MCD の発症はほとんど AIDS 患者に限られ，AIDS と関連しない症例では HHV-8 は通常，検出されない (Soulier ら，1995[3]；Suda ら，2001[4])．AIDS 関連の MCD はほとんどが HHV-8 陽性で，PEL と同じ危険因子の患者（AIDS，男性同性愛者，Kaposi 肉腫合併）に発症する．HHV-8 陽性 MCD では血清中に vIL-6 が発現し，リンパ濾胞暗殻に HHV-8 感染細胞が検出される (Katano ら，2000[5])．

2 HHV-8 関連 MCD の HE 染色

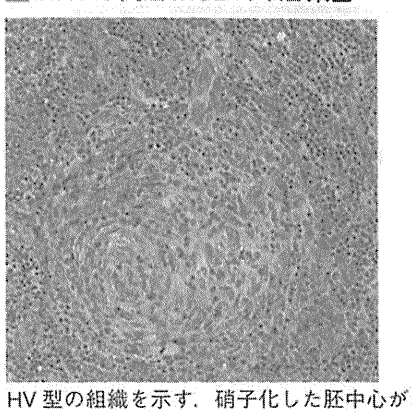

HV 型の組織を示す．硝子化した胚中心がみられ，暗殻は同心円状に拡大している．胚中心に向かって伸びる血管が特徴的である．

HHV-8 関連多巣性 Castleman 病に発症する大細胞性 B 細胞リンパ腫

HHV-8 関連の多巣性 Castleman 病（MCD）から発症するリンパ腫（large B-cell lymphoma arising in HHV-8-associated multicentric Castleman disease）であり，PEL と同じ危険因子の患者（AIDS，男性同性愛者，Kaposi 肉腫合併）に発症する (Isaacson ら，2008[6])．形態的に plasma cell に似ることから HHV-8-positive plasmablastic lymphoma ともいわれる．MCD を発生母地とすることから，リンパ節や脾臓に発症し，リンパ節腫脹や脾腫として現れる．

組織学的には Castleman 病の病変部の mantle zone および濾胞間に plasma cell 様の細胞が小さな集塊を形成する像がみられる．免疫組織学的にはこれらの細胞は HHV-8 LANA-1 が陽性で，HHV-8 の溶解性感染関連蛋白である vIL-6 も多くの細胞で陽性である．cIgM，λ 軽鎖が陽性である点は PEL とは異なる．Castleman 病の存在が extracavity PEL との鑑別には重要である．

（片野晴隆，佐多徹太郎）

▶文献は巻末に収載

Virology xxx (2012) xxx–xxx

Contents lists available at SciVerse ScienceDirect

Virology

journal homepage: www.elsevier.com/locate/yviro

Novel monoclonal antibodies for identification of multicentric Castleman's disease; Kaposi's sarcoma-associated herpesvirus-encoded vMIP-I and vMIP-II

Kazushi Nakano [a,1], Harutaka Katano [c,1], Kenjiro Tadagaki [b], Yuko Sato [c], Eriko Ohsaki [a], Yasuko Mori [d,e], Koichi Yamanishi [e], Keiji Ueda [a,*]

[a] Division of Virology, Department of Microbiology and Immunology, Osaka University Graduate School of Medicine, 2-2 Yamada-oka, Suita, Osaka 565-0871, Japan
[b] Institut Cochin, Université Paris Descartes, CNRS (UMR 8104) Inserm U1016, Paris, France
[c] Department of Pathology, National Institute of Infectious Diseases, Tokyo, Japan
[d] Division of Clinical Virology, Kobe University Graduate School of Medicine, 7-5-1, Kusunoki-cho, Chuo-ku, Kobe, 650-0017, Japan
[e] Division of Biomedical Research, National Institute of Biomedical Innovation, Ibaraki, Osaka, Japan

ARTICLE INFO

Article history:
Received 29 August 2011
Returned to author for revision 2 October 2011
Accepted 11 January 2012
Available online xxxx

Keywords:
Kaposi's sarcoma-associated herpesvirus
Kaposi's sarcoma
Multicentric Castleman's disease
Viral macrophage inflammatory protein
vMIP-I
vMIP-II
Chemokine
KSHV
HHV-8

ABSTRACT

Recent studies have indicated that vMIP-I and vMIP-II play important roles in the pathogenesis of Kaposi's sarcoma-associated herpesvirus (KSHV)-related diseases due to the effects of these proteins on vascularization. We developed monoclonal antibodies against KSHV-encoded viral macrophage inflammatory protein-I (vMIP-I) and vMIP-II to study these expression profiles and reveal the pathogenesis of KSHV-related diseases. The MAbs against vMIP-I and vMIP-II reacted to KSHV-infected cell lines after lytic induction. Both vMIP-I and the vMIP-II gene products were detected 24 h post-induction with 12-*O*-tetradecanoylphorbol-13-acetate until 60 h in the cytoplasm of primary effusion lymphoma cell lines. In clinical specimens, both vMIP-I and vMIP-II gene products were detected in the tissues of patients with multicentric Castleman's disease. On the other hand, only vMIP-II was detected in a subset of Kaposi's sarcoma. We concluded that these antibodies might be powerful tools to elucidate the pathogenesis of KSHV-related diseases.

Introduction

Kaposi's sarcoma-associated herpesvirus (KSHV), also known as human herpesvirus 8 (HHV-8), is a gammaherpesvirus originally identified in HIV-positive Kaposi's sarcoma (KS) tissues (Chang et al., 1994). KSHV is responsible for AIDS associated cancers such as Kaposi's sarcoma (KS), primary effusion lymphoma (PEL), and multicentric Castleman's disease (MCD) (Cesarman et al., 1995; Schalling et al., 1995; Soulier et al., 1995). As is the case for all herpesviruses, KSHV has two life cycles, one latent and the other lytic. Lytic gene expression can be induced by the treatment of latently infected cells with chemical agents such as 12-*O*-tetradecanoylphorbol-13-acetate (TPA), sodium butyrate (Arvanitakis et al., 1996; Miller et al., 1997). It has been demonstrated that two KSHV-encoded chemokines, K6 (which encodes a vMIP-I) and K4 (which encodes a vMIP-II), are expressed in the course of lytic infection (Moore et al., 1996; Sun et al., 1999). Previous reports showed that both vMIP-I and vMIP-II induced Ca^{2+} signal transduction via certain chemokine receptors and the receptor-dependent migration of cells (Benelli et al., 2000; Chen et al., 1998; Endres et al., 1999; Kledal et al., 1997). In addition, in a chick chorioallantoic membrane assay, the both proteins showed strong angiogenic properties (Boshoff et al., 1997). However, little is known about the contribution of vMIPs to KSHV malignancy under physiologic conditions.

In this report, we generated new monoclonal antibodies against vMIP-I and vMIP-II, and confirmed the detection of both vMIP-I and vMIP-II in histological sections of tissues from MCD patients as well as in KSHV-infected PEL cell lines. In cases of KS, vMIP-II was detected, but not vMIP-I. These results suggest that the expression properties of vMIP-I and vMIP-II might be related to KSHV-associated diseases, and may even be involved in the generation of diseases. Thus, antiviral chemokine MAbs could potentially become useful tools for the diagnosis of KSHV-related diseases.

Materials and methods

Cells

Kaposi's sarcoma-associated herpesvirus-positive cell lines (BC-1, BC-3, BCBL-1 and TY-1 cells) and a negative cell line (BJAB cells) were

* Corresponding author. Tel.: +81 6 6879 3780; fax: +81 6 6879 3789.
E-mail address: kueda@virus.med.osaka-u.ac.jp (K. Ueda).
[1] Equal contribution by these authors.

0042-6822/$ – see front matter © 2012 Elsevier Inc. All rights reserved.
doi:10.1016/j.virol.2012.01.008

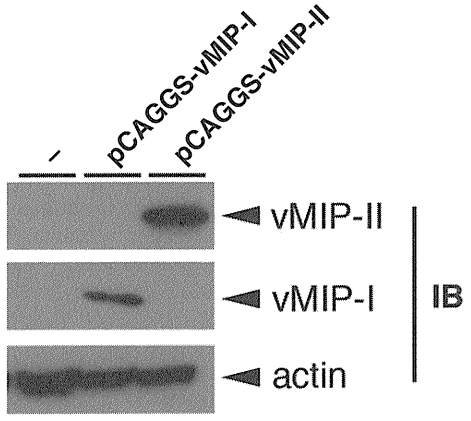

Fig. 1. Cross reactivity between anti-vMIP-I and anti-vMIP-II MAb. 293 T cells were transfected with either 2 μg of pCAGGS- vMIP-I or 2 μg of pCAGGS-vMIP-II plasmids. Forty-eight hours after transfection, the cells were harvested and expression of vMIP-I or vMIP-II was tested by Western blot analysis using the anti-vMIP-I or -vMIP-II MAb, respectively. Actin was also probed with anti-actin monoclonal Ab as a loading control.

obtained from the American Type Culture Collection (ATCC) (Manassas, VA). These cells were grown in RPMI 1640 (Nakalai Tesque, Inc., Kyoto, Japan) supplemented with 10 IU/ml penicillin G, 10 μg/ml streptomycin, 10% heat-inactivated fetal bovine serum (FBS) (HyClone, Logan, UT) in a 5% CO_2 atmosphere. In addition, 293 T and 293/EBNA (Clontech) cells were grown in Dulbecco's modified Eagle's medium (DMEM) (Nakalai Tesque, Inc.) supplemented with 10 IU/ml penicillin G, and 10 μg/ml streptomycin, 10% FBS, and 200 mM L-glutamine.

Plasmids

In order to express vMIP-I and vMIP-II, the ORFs were cloned into the pCAGGS eukaryotic expression vector, and pCAGGS-vMIP-I and pCAGGS-vMIP-II were established. The plasmid vector, pCAGGS was kindly provided by Dr. J. Miyazaki of Osaka University (Niwa et al., 1991). Briefly, fragments including vMIP-I and vMIP-II ORFs were amplified by PCR using the following primer sets: vMIP-I-Met (5′-CGGTACCGAATTCTCCAGATGGCC-3′) and vMIP-I-Ter (5′-ACTCGAGAATTCTACTTGTCATCGTCGTCCTTGTAGTCGGAAGCTATGGCAGGCAG-3′); and vMIP-II-Met (5′-AGGTACCGAATTCAGTTATGGACACCAAGGGC-3′) and vMIP-II-Ter (5′-ACTCGAGAATTCTACTTGTCATCGTCGTCCTTGTAGTCGGAGCGAGCAGTGACTGG-3′). The PCR products were cloned into pCR2.1 (Invitrogen) and sequenced. After digestion with *Eco*RI, the fragments were ligated into the *Eco*RI site of the pCAGGS vector. Then, the DNA fragments encoding vMIP-I and vMIP-II were liberated by *Eco*RI, and were inserted into pCAGGS to generate the expression vectors pCAGGS-vMIP-I and -vMIP-II, respectively. vMIP-I (pGEX-vMIP-I) and vMIP-II (pGEX-vMIP-II) were also generated using PCR-based technology using BCBL-1 genomic DNA as a templete. The coding region, without a signal peptide, was amplified with vMIP-I-Eco (CAGAATTCGCGGGGTCACTCGTGTCG-3′), vMIP-I-Sal (CTGTCGACCGTCTAAGCTATGGCAGG-3′), vMIP-II-Eco (5′-CGGAATTCGCGTCCTGGCATAGACCG-3′), and vMIP-II-Sal (5′-GGGTCGACATTCTTCAGCGAGCAGTG-3′). The amplified vMIP-I and the vMIP-II fragments were digested with *Eco*RI and *Sal*I and inserted downstream of the GST coding of pGEX-5X-1 (GE Healthcare, Uppsala, Sweden) at the *Eco*RI and *Sal*I sites to construct pGEX-vMIP-I and pGEX-vMIP-II. To express a full-length and the deletion mutants of the GST-vMIP-I and GST-vMIP-II fusion protein, the genes for GvM1-Full, GvM1-D1, GvM1-D2,

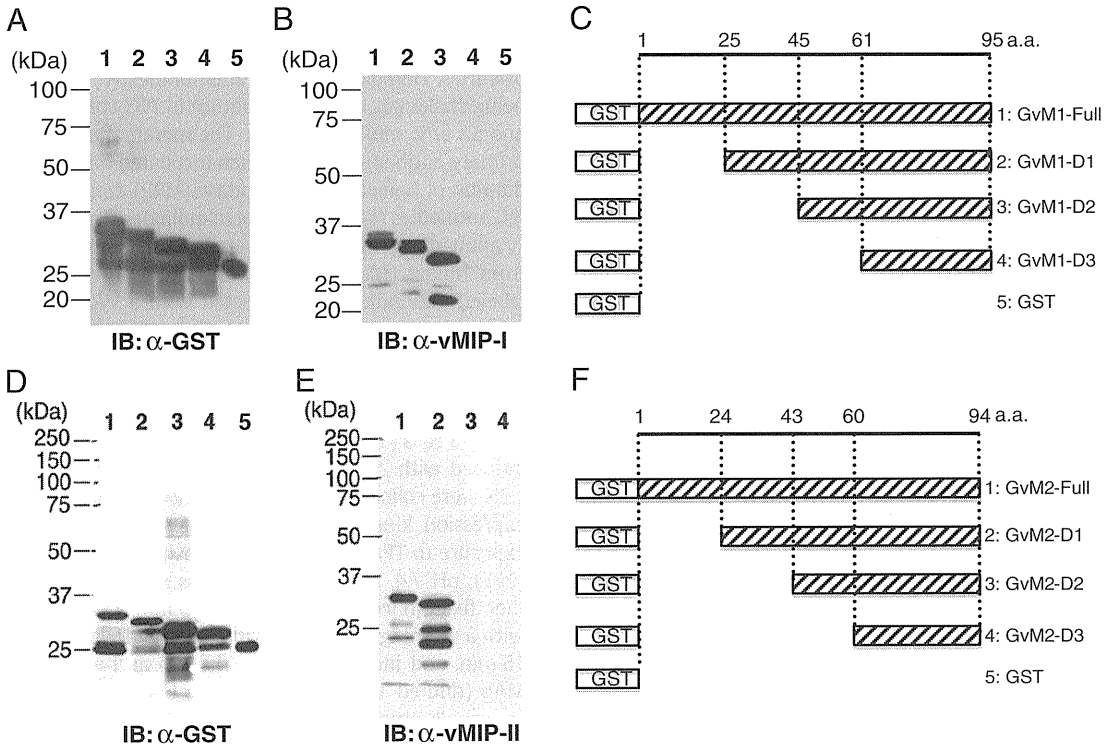

Fig. 2. Epitope mapping of the anti-vMIP-I and the anti-vMIP-II MAbs. To map the regions of vMIP-I and vMIP-II recognized by the anti-vMIP-I and anti-vMIP-II antibody, a series of GST-vMIP-I and GST-vMIP-II fusion proteins containing the individual regions of vMIP-I and vMIP-II were constructed as described in Fig. 2C and F, and the proteins were expressed in *E. coli*. The lysates of the fusion proteins, vMIP-I and vMIP-II, and its deletion mutants were immunoblotted with an anti-GST antibody (A and D) and an anti-vMIP-I (B) and an anti-vMIP-II antibody (E) to detect GST-vMIP-I or GST-vMIP-II fusion proteins. Lane 1, GvM1-Full; lane 2, GvM1-D1; lane 3, GvM1-D2; lane 4, GvM1-D3; lane 5, GvM1-D4; lan3 6, GST in Fig. 2A and B. Lane 1, GvM2-Full; lane 2, GvM2-D1; lane 3, GvM2-D2; lane 4, GvM2-D3; lane 5, GST (in D only) in Fig. 2D and E. Summary of GST-vMIP-I (C) and GST-vMIP-II (F) deletion mutants. Individual regions of vMIP-I and vMIP-II were cloned in-frame into the pGEX-5X-1 vector to generate GST-vMIP-I and GST-vMIP-II fusion proteins, respectively. The boxes at left indicate GST, and the white boxes with slashed lines indicate individual domains of vMIP-I and vMIP-II. 1, GvM1-Full(1-95a.a.); 2, GvM1-D1(25-95a.a.); 3, GvM1-D2(45-95a.a.); 4, GvM1-D3(61-95a.a.) in Fig. 2C, and 1, GvM2-Full(1-94a.a.); 2, GvM2-D1(24-94a.a.); 3, GvM2-D2(43-94a.a.); 4, GvM2-D3(60-94a.a.) in Fig. 2F.

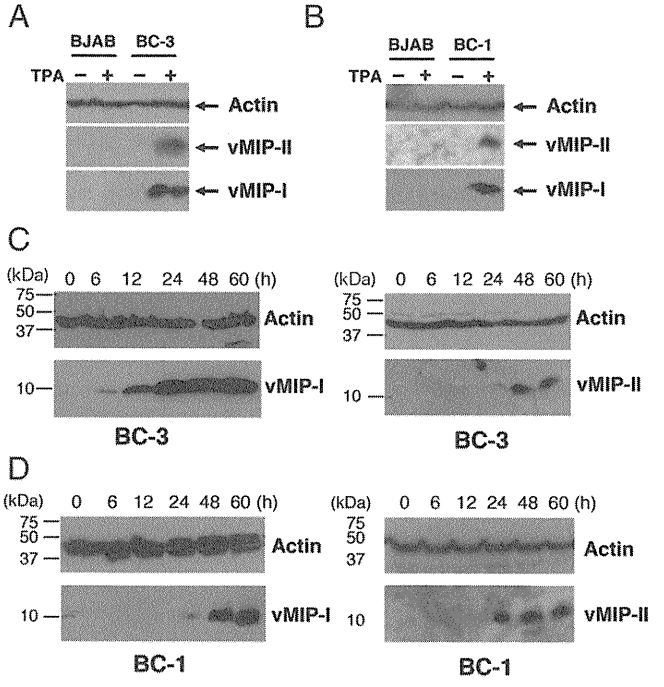

Fig. 3. Detection of vMIP-I and vMIP-II gene products in a KSHV-infected PEL cell line. BC-1 and BC-3 cells were treated with TPA for the indicated number of hours, and the whole-cell extract was prepared after the indicated time post-induction. vMIP-I and vMIP-II were detected by Western blotting and IFA with anti-vMIP-I and -vMIP-II antibodies. Western blot analysis of protein extracted from BC-3 and BJAB cells (A), and BC-1 and BJAB cells (B) with either the anti-vMIP-I or the anti-vMIP-II MAb. Arrows indicate actin, vMIP-I, and vMIP-II proteins. As expected, the estimated sizes of the vMIP-I and vMIP-II proteins, based on comparisons with the migration of molecular size markers, was around 10 kDa. Expression kinetics of vMIP-I (left panel) and vMIP-II (right panel) in TPA-treated BC-3 (C) and BC-1 (D) cells by Western blot analysis. BC-1 and BC-3 cells were harvested after 6, 12, 24, 48, and 60 h post-induction. The lysate was subjected to Western blot analysis as in (A).

GvM1-D3, GvM2-Full, GvM2-D1, GvM2-D2, and GvM2-D3 genes were generated by PCR using the following primer sets: vMIP-I-1F (5′-ATGAATTCCAGATGGCCCCCGTCCAC-3′) and vMIP-I-5R (5′-CCGTGTCGACCGTCTAAGCTATGGCAGGCAGC-3′); vMIP-I-2F (5′-ATGAATTCGCGGGGTCACTCGTGTCG-3′) and vMIP-I-5R; vMIP-I-3F (5′-ATGAATTCCCGCCCGTCCAAATTC-3′) and vMIP-I-5R; vMIP-I-4F (5′-ATGAATTCCCAAAACCCGGAGTTATTTTGC-3′) and vMIP-I-5R; vMIP-II-1F (5′-CGGAATTCGTTATGGACACCAAGGGC-3′) and vMIP-II-5R (5′-GGCAGTCGACTCTTCAGCGAGCAGTGACTG-3′); vMIP-II-2F (5′-GGGAATTCCTGGGAGCGTCCTGGCATAGAC-3′) and vMIP-II-5R; vMIP-II-3F (5′- AAGAATTCTTACCACAGGTGCTTCTGTCC-3′) and vMIP-II-5R; and vMIP-II-4F (5′-TGGAATTCAAGCCGGGTGTGATATTTTTG-3′) and vMIP-II-5R. The PCR products were cloned into pCR2.1 (Invitrogen, Carlsbad, CA) and confirmed by sequencing. The products were digested with the *Eco*RI and *Sal*I restriction enzymes and were cloned into pGEX-5X-1 (GE Healthcare). The PCR conditions for all products were as follows: 25 cycles of 94 °C for 1 min, 55 °C for 1 min, and 72 °C for 2 min in a TP480 PCR thermal cycler (Takara Shuzo, Kyoto, Japan).

Immunization and generation of monoclonal Abs against vMIP-I and vMIP-II

In mice, anti-vMIP-I and -vMIP-II antibodies were raised against the GST-vMIP-I and GST-vMIP-II fusion protein, respectively. These GST fusion proteins were purified on a glutathione-Sepharose 4B column (GE Healthcare), and the GST-vMIP-I and the GST-vMIP-II fusion proteins were conjugated to keyhole limpet hemocyanin KLH (Calbiochem. Co., La Jolla, CA). Mice were initially immunized with 250 μg each of the purified GST-vMIP-I or -II fusion protein in Freund's complete adjuvant administered to the peritoneal cavity, and 200 μg of the antigen in Freund's incomplete adjuvant were injected again 14 and 28 days after the first injection. The mice were exsanguinated 7 days after the last injection. To generate MAbs against vMIP-I and vMIP-II, hybridomas were established by fusing splenocytes from the hyperimmune mice using a nonproducing myeloma cell line, Sp-2/0-Ag14 (ATCC, Manassas, VA). After selection in medium containing hypoxanthine-aminopterin-thymidine, cells secreting MAbs were screened by immunofluorescence assays (IFA). The TPA-induced and -uninduced BCBL-1 cells were fixed in acetone and exposed to supernatants of the hybrid cells. Clones secreting antibodies reactive with TPA-stimulated BCBL-1 cells were expanded and isolated by limiting dilutions.

Transfection analysis of vMIP-I and vMIP-II

To express the vMIP-I and vMIP-II proteins, 293/EBNA cells were transfected with pCAGGS-vMIP-I and -vMIP-II plasmids using TransIT-LT1 (Mirus Bio LLC, Madison, WI). The transfected cells were incubated for 48 h in DMEM supplemented with 10% FCS. The cells were harvested and lysed with lysis buffer (0.05 M Tris-HCl [pH 8.0], 0.15 M NaCl, 0.5% sodium deoxycholate, 1% Triton X-100, 0.1% sodium-dodecyl sulfate [SDS]). The cell lysate was fractionated by electrophoresis on 16% polyacrylamide gel as described below.

Antibodies and Western blotting

The expression of vMIP-I and vMIP-II in BC-3 cells stimulated with TPA was determined with MAbs against vMIP-I and vMIP-II, respectively, as noted above. The concentration of proteins extracted from BC-3 cells was normalized using a BCA Protein Assay Kit (Thermo Fisher Scientific Inc., Rockford, IL). The samples were subjected to SDS-15% polyacrylamide gel electrophoresis under reducing conditions, and were electrophoretically transferred to PVDF membranes (Bio-Rad Laboratories, Hercules, CA). The membranes were blocked for 1 h while being shaken at room temperature in PBS containing 0.05% Tween 20 and 5% w/v nonfat skim milk. The membranes were incubated with a primary antibody and were then incubated for 1 h with an appropriate dilution of horseradish peroxidase (HRP)-conjugated goat anti-mouse IgG antibodies (Santa Cruz Biotechnologies, Santa Cruz, CA). The primary antibody against actin, anti-actin (Ab-1) mouse MAb, was purchased from Merck (Merck KGaA, Darmstadt, Germany). The bound HRP-labeled antibodies were detected with a West Pico substrate kit for horseradish peroxidase (Thermo Fisher Scientific Inc).

IFA

BC-3 cells (10^7 cells) in RPMI 1640 medium with supplements were induced with 25 ng/ml TPA (Sigma Chemical Co., St. Louis, MO). The cells were collected after 0, 4, 8, 12, 24, 48, and 60 h for analysis of the expression kinetics, and for cellular localization analysis 48 h after exposure to TPA. The cells were washed in phosphate-buffered saline (PBS), pH 7.4, and spotted on glass slides. The spots were air-dried, then fixed in ice-cold acetone for 10 min. The cells were then washed with a washing buffer (PBS supplemented with 0.1% Triton X-100) for 15 min, and incubated with either an anti-vMIP-I or an anti-vMIP-II MAb (diluted 1:100 in IFA dilution buffer [PBS containing 2% bovine serum albumin, 0.2% Tween-20, and 0.05% NaN_3]) for 1 h at 37 °C. Then, the slides were washed with the washing buffer, and incubated for 1 h at room temperature with a pre-standardized diluted fluorescein isothiocyanate (FITC)-conjugated goat anti-mouse IgG (Tago Immunologicals, Camarillo, CA). The slides were washed and stained with 4′, 6′-diamidino-2-phenylindole (DAPI) to detect nuclei and were mounted with 50% (v/v) glycerol in PBS. For formalin-fixed paraffin-embedded tissues, antigen retrievals were performed on the de-paraffined sections using citrate buffer. Alexa 488 or 568-conjugated

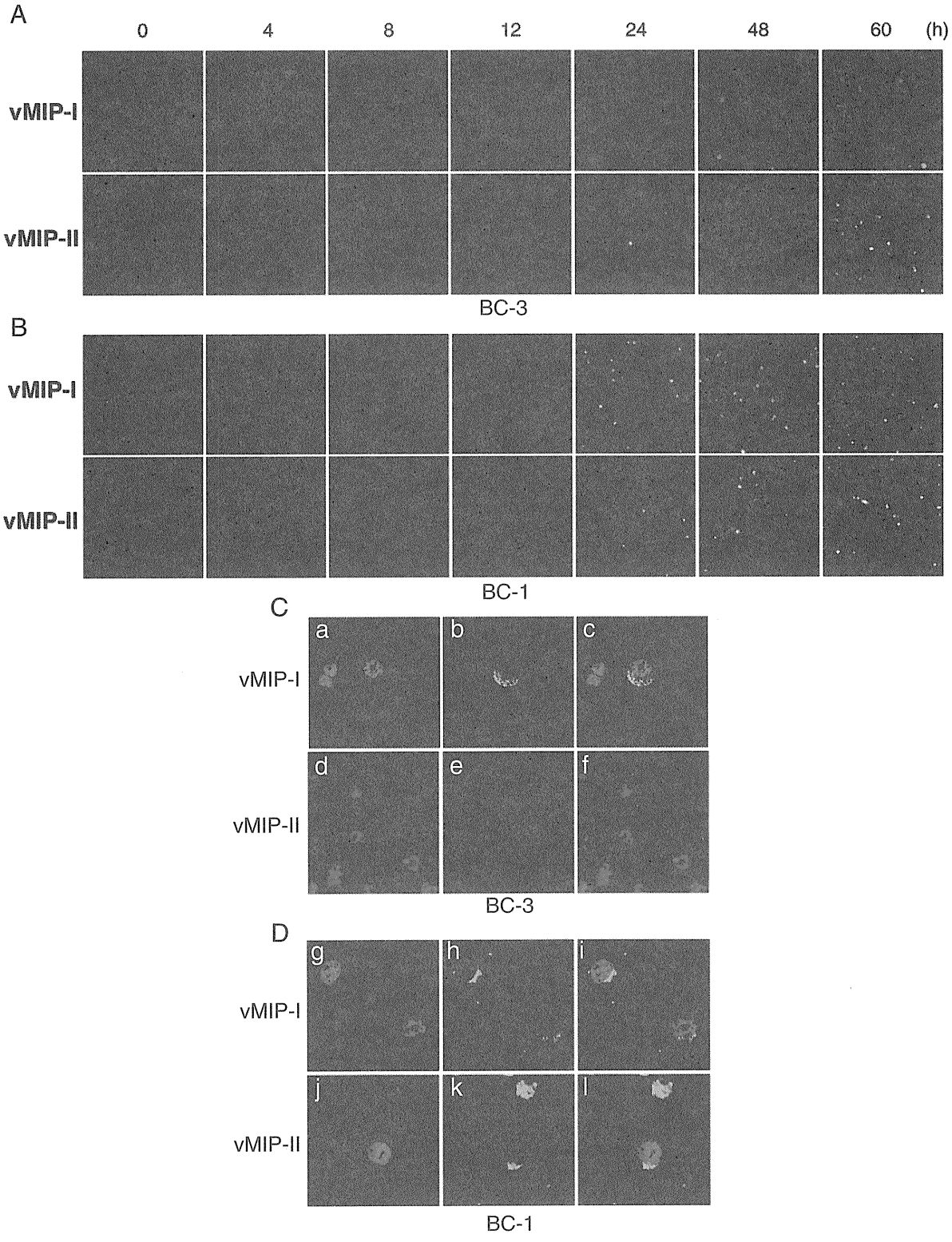

Fig. 4. Expression of vMIP-I and vMIP-II in BC-3 and BC-1 cells by IFA. After 4, 8, 12, 24, 48, and 60 h, BC-3 (A) and BC-1 (B) cells were labeled either with the anti-vMIP-I (upper) or the anti-vMIP-II (lower) MAb followed by goat anti-mouse FITC-conjugated Abs. FITC photomicrographs showing anti-vMIP-I and anti-vMIP-II immunoreactivity in BC-3 and BC-1 cells treated with TPA. (C) Cellular localization of vMIP-I and vMIP-II in BC-3 (C) and BC-1 (D) cells. The cells were stained with DAPI (a, d, g and j), and the localization of vMIP-I and vMIP-II was visualized by IFA with anti-vMIP-I or -vMIP-II MAbs (b, e, h and k); panel a and b, d and e, g and h, and j and k were merged (c, f, i and l). Fluorescence photomicrographs revealed anti-vMIP-I and -vMIP-II immunoreactivity using FITC-conjugated anti-mouse IgG MAb.

anti-mouse or rabbit antibodies (Invitrogen) were used as the secondary antibodies. Confocal microscopic analysis was performed (FV-1000, Olympus, Tokyo, Japan), and the contrast was adjusted before the images were exported as TIFF files to Adobe Photoshop.

Immunohistochemistry

Formalin-fixed paraffin-embedded tissues from KS and MCD patients, and those from an animal model of KSHV-associated solid lymphoma

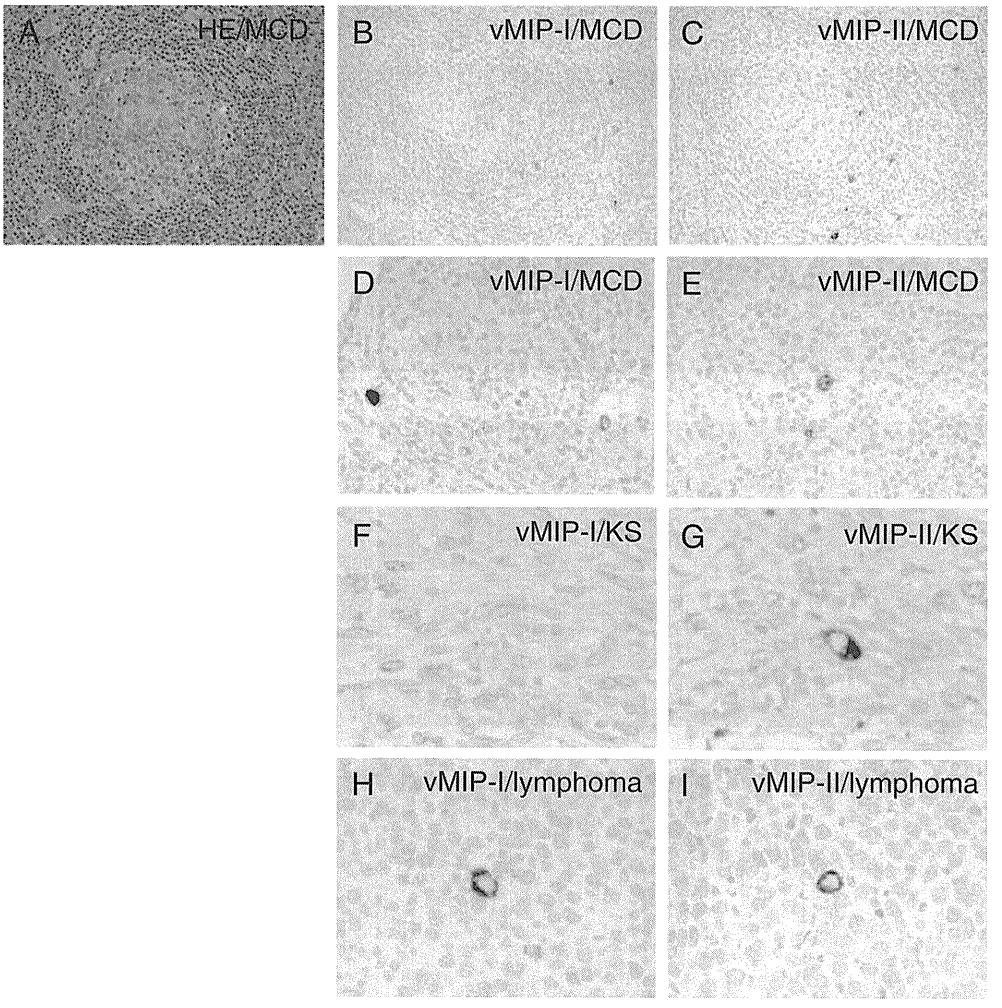

Fig. 5. Expression of vMIP proteins in KSHV-associated diseases. (A–C) Hematoxylin and eosin staining and immunohistochemistry for vMIPs in serial sections of a tissue sample from a patient with MCD. Brown stains indicate positive signals. The nucleus was counter-stained by hematoxylin. (D and E) Higher magnification view of vMIPs expression in an MCD case. Some large lymphocytes in the mantle zone were stained. (F and G) vMIP-I and vMIP-II expression in a KS sample. (H and I) Expression of vMIPs in an animal model of KSHV-associated lymphoma in SCID mice.

were sectioned and stained with hematoxylin and eosin (H&E). Immunohistochemistry of the serial sections was performed with either the anti-vMIP-I or -II MAb. For the second- and third- phase reagents used for immunostaining, a CSAII kit (DAKO, Copenhagen, Denmark) was used. An animal model of KSHV-associated solid lymphoma, which was established as described previously (Katano et al., 2000b), was also subjected to immunohistochemical analysis. Briefly, TY-1 cells were inoculated into the subcutaneous tissue of mice with severe combined immunodeficiency (SCID). One month after inoculation, lymphomas appeared in the subcutaneous region at the inoculation site. Lymphoma cells contained the KSHV genome, and expressed various viral proteins of KSHV (Katano et al., 2000b).

Table 1
Expression of vMIP-I and vMIP-II in MCD and KS tissue samples.

	KSHV proteins, (+)/total	
Cases	vMIP-I	vMIP-II
MCD	(3)/3	(3)/3
KS	(0)/5	(2)/8

Chemotaxis assays

Chemotaxis assays were performed as described previously (Nakano et al., 2003). Briefly, THP-1 cells were washed twice with chemotaxis buffer, 0.5% bovine serum albumin, 20 mM HEPES, pH 7.4, in RPMI 1640. Migration of cells was assessed in a cell culture chamber (Costar, Cambridge, MA), with the upper and lower compartments separated by a 3 μm pore size polycarbonate filter (???). The lower compartment of the chamber was filled with dilutions of vMIP-I, vMIP-II (R&D Systems, Minneapolis, MN) or with PBS alone, and/or with each 10 μg/ml anti-vMIP-I or -vMIP-II MAbs at a volume of 600 μl. The upper compartment contained 100 μl of THP-1 cell suspensions in chemotaxis buffer (10^5 cells/well). The chambers were then incubated for 4 hours at 37 °C, 5% CO_2, and spun at 300 x g, 4 °C, for 5 min. Finally, the cells from the lower compartment were counted.

Results

Specificity of the anti-vMIP-I MAb and the anti-vMIP-II MAb

In order to check specificity of the MAbs, we transfected vMIP-I and vMIP-II expression vectors (pCAGGS-vMIP-I, and -II) into 293/EBNA

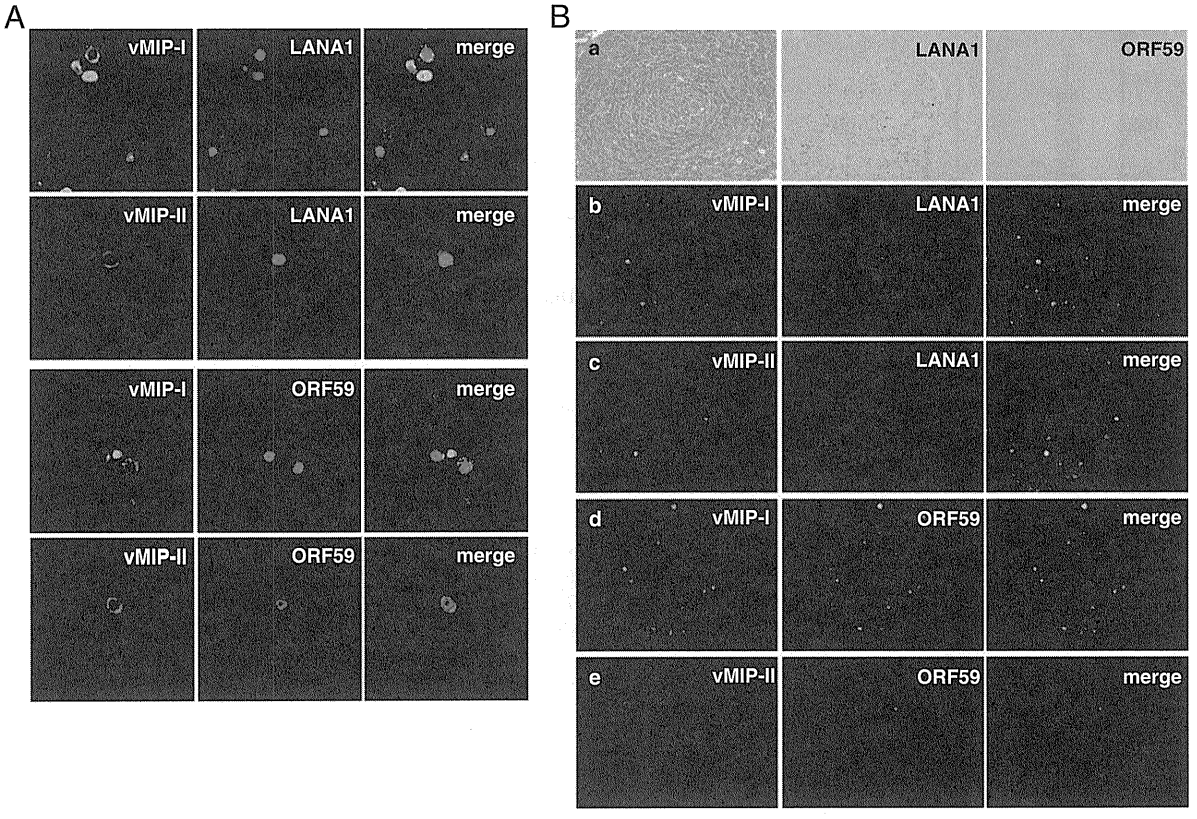

Fig. 6. (A) Expression of vMIPs. LANA1 and ORF59 in the animal model of KSHV-associated solid lymphoma by confocal microscopy. vMIPs were labeled with Alexa 488 (green). LANA1 (upper panels) and ORF59 (lower panels) were labeled with Alexa 568 (red). (B) Expression of vMIPs in MCD. (a) HE staining and immunohistochemistry of LANA1 and ORF59. (b–e) Immunofluorescence assay on MCD lesion. A germinal center is shown in the center of each panel. This case is KSHV-positive large B cell lymphoma arising in MCD (for interpretation of the color references in this article, the reader is referred to the online version).

cells, respectively. The total lysate of the transfected cells was subjected to Western blot analysis. vMIP-I and vMIP-II proteins were detected with anti-vMIP-I or vMIP-II MAbs, respectively (Fig. 1). These antibodies did not show cross-reactivity each other.

Epitope mapping of the anti-vMIP-I and anti-vMIP-II MAbs

We established hybridoma clones secreting MAbs against vMIP-I and vMIP-II, respectively. To map the regions of vMIP-I and vMIP-II where anti-vMIP-I and anti-vMIP-II antibody reacted, a series of GST-fused vMIP-I and vMIP-II deleted proteins were constructed as described in Fig. 2C and F, and used for Western blot analysis with an anti-GST antibody (Santa Cruz Biotechnology Inc), (Fig. 1A, D) and the anti-vMIP-I or the anti-vMIP-II (Fig. 1B, E) antibody, respectively. The results showed that all GST-vMIP-I and GST-vMIP-II fusion proteins interacted with the anti-GST antibody (Fig. 2A, D) and showed that GvM1-Full, GvM1-D1, and GvM1-D2 reacted with the anti-vMIP-I antibody, whereas GvM1-D3 did not (Fig. 1B), and GvM2-Full and GvM2-D1 reacted with the anti-vMIP-II antibody, whereas GvM2-D2, and GvM2-D3 did not (Fig. 2E). Thus, these results demonstrated that an anti-vMIP-I MAbs was successfully generated and suggest that the amino acid residues 61 to 95 of vMIP-I could be a major epitope reacted with the anti-vMIP-I antibody. On the other hand, the amino acid residues 24 to 42 of vMIP-II could be an epitope reacted with the anti-vMIP-II antibody.

Expression of vMIP-I and vMIP-II in the KSHV-infected PEL cell line

We tested vMIP-I and vMIP-II expression in KSHV and Epstein Barr virus (EBV) dually infected PEL cell lines (BC-1), KSHV infected PEL cell lines (BC-3) and in non-infected Burkitt's lymphoma cell line (BJAB), and detected them in TPA-stimulated BC-3 and BC-1 cells with developed antibodies, but not in BJAB cells non-stimulated BC-3 or BC-1 cells (Fig. 2A, B). In a KSHV infected PEL cells, BC-1 and BC-3, vMIP-I and vMIP-II were detected around at 10 kDa, which matches the size deduced from amino acids length (Fig. 3C, D). Actually, vMIP-I was detected from 6 hours post induction and vMIP-II was at 24 hours in BC-3 cells (Fig. 3C), and vMIP-I and vMIP-II were detected at 24 h in BC-1 cells (Fig. 3D). In the immunofluorescence microscopy, the number of vMIP-II expressing cells seemed to be more than that of vMIP-I in BC-3 cells (Fig. 4A, B). In order to analyze the cellular localization of vMIP-I and vMIP-II protein, BC-3 and BC-1 cells stimulated with TPA were doubly labeled with DAPI (Fig. 4C, a, d and D, g, j), and either the anti-vMIP-I MAb (Fig. 4C, b and D, h) or the anti-vMIP-II MAb (Fig. 4C, e and D, k). Merged images were shown in Fig. 4C, c, f, and D, i, l). The vMIP-I and the vMIP-II clearly showed cytoplasm and possibly membranes in TPA-induced BC-3 and BC-1 cells (Fig. 4C, b, e, and D, h, k).

Expression of vMIPs in KSHV-associated diseases

To know the expression of vMIPs in KSHV-associated diseases, immunohistochemistry for vMIPs was performed on pathological samples of eight KS cases, three MCD cases, and the animal model of KSHV-associated solid lymphoma (Fig. 5). Immunohistochemistry demonstrated that vMIP-I and vMIP-II were detected in some cells in the mantle zone of germinal center and the interfollicular zone in KSHV-positive MCD samples (Fig. 5A to E). Both vMIP-I and vMIP-II were detected predominantly in the cytoplasm of large lymphocytes. The numbers of positive cells varied among three MCD cases examined. On the other

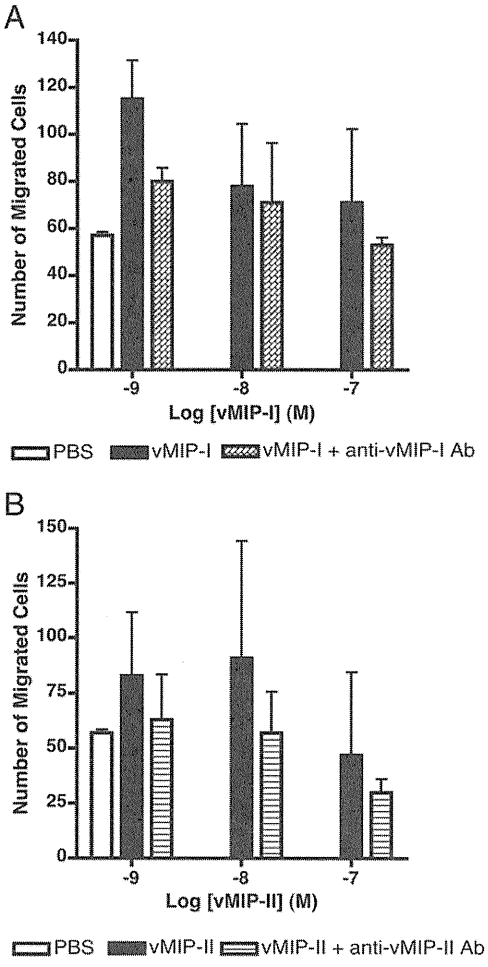

Fig. 7. Neutralizing activity of anti-vMIP-I and -vMIP-II MAbs. THP-1 cell migration in response to increased concentrations of vMIP-I and vMIP-II (1, 10, 100 nM), and the neutralizing activity of 10 μg/ml anti-vMIP-I and -vMIP-II MAbs against vMIP-I and vMIP-II were measured, as outlined in Materials and Methods, by using the transwell migration assay system. Various doses of vMIP-I and vMIP-II were tested for their ability to induce the chemotaxis of THP-1 cells. The data presented are from one experiment, and are representative of the triplicate experiments performed. The error bars indicate the standard deviations of three independent experiments.

hand, any positive signal of vMIP-I was not observed in all KS cases (Fig. 5F, G). vMIP-II was rarely detected in the cytoplasm of spindle cells in two KS cases at the nodular stage out of eight KS cases. In the samples of animal model of KSHV-associated solid lymphoma, both vMIP-I and vMIP-II were detected in the cytoplasm of a part of lymphoma cells (Fig. 5H, I). These data showed that vMIP-I and vMIP-II were expressed in cells in MCD and KSHV-associated lymphoma, but vMIP-II was rarely in KS (Table 1). To know the association of vMIPs expression with expression of other KSHV-encoded proteins, we examined immunofluorescence assay on KSHV-associated diseases. Since, all KSHV-infected cells express LANA1, vMIPs-positive cells were positive for LANA1. However, expression pattern of LANA1 showed diffuse nuclear staining in vMIPs-positive cells in the animal model of KSHV-associated solid lymphoma (Fig. 6A). Confocal microscopy revealed that vMIP-I stain showed usually cytoplasmic pattern, but rarely diffuse nuclear staining pattern *in vivo*. Almost all cells with vMIPs expression were also positive for ORF59 protein, a lytic protein of KSHV. IFA also demonstrated that vMIPs-positive cells expressed LANA1 at various levels in MCD clinical samples (Fig. 6B, a to c). A large portion of vMIPs-positive cells also expressed ORF59 protein in MCD (Fig. 6B, d, e). These data suggest that vMIPs are expressed by cells with KSHV-lytic infection in KSHV-associated MCD and lymphoma.

Neutralization of vMIP-I and vMIP-II by anti-vMIP-I and anti-vMIP-II MAbs

We examined whether the anti-vMIP-I and anti-vMIP-II MAbs could neutralize the chemoattractant of vMIP-I and vMIP-II to induce the migration of THP-1 cells. As expected, vMIP-I and vMIP-II induced migration of THP-1 cells (Fig. 7A, B), but not with PBS alone. However, anti-vMIP-I and anti-vMIP-II MAbs inhibited respective vMIP-I and vMIP-II-induced cell migration of THP-1 cells at 10 μg/ml final concentration.

Discussions

It was known that KSHV encodes three chemokine genes of the so-called viral macrophage inflammatory proteins: *vMIP-I*, *vMIP-II*, and *vMIP-III* in the genome. Analysis of the translated amino acid sequence indicate that the vMIP-I and vMIP-II gene have four conserved cysteines capable of forming two essential disulfide bonds (first cysteine and third cysteine, and second cysteine and fourth cysteine). The family of chemokines comprises CC, CXC, C, and CX_3C subfamilies. The vMIP-I and vMIP-II have four cysteines, the first two of which are found in the sequence of CC, which correspond to the CC profile. These gene products were expressed in the phase of KSHV lytic infection (Moore et al., 1996; Sun et al., 1999). Both vMIP-I and vMIP-II were expressed in a KSHV-infected cell lines, BC-3, which had been treated with TPA. Mono-specific polyclonal Abs against vMIP-I and vMIP-II have been described in previous studies that investigated the localization of vMIPs in PEL cells (Nakano et al., 2003). In the present study, we developed the respective MAbs that reacted either with KSHV vMIP-I or vMIP-II. We first applied these MAbs against KSHV vMIP-I and vMIP-II to detect KSHV-infected BC-3 and BC-1 cells by Western blotting and immunofluorescence assay. The Western blot analysis revealed that both the anti-vMIP-I and the anti-vMIP-II MAbs reacted to the 10-kDa proteins considered specific to the respective vMIP protein. The anti-vMIP-I MAb was shown to be reactive with the epitopes in the middle of the protein (sequence, PPVQILKEWYPTSPAC), and the epitope of the anti-vMIP-II MAb was shown to be reactive at the N-terminal end (sequence, LGASWHRPDKCCLGYQKRP). Further immunofluorescence analysis of the cellular localization of both vMIP-I and vMIP-II with anti-vMIP-I and anti-vMIP-II MAb showed a cytoplasmic pattern of expression in BC-3 and BC-1 cells. As the results indicated that these gene products were expressed in the cytoplasm, it might be located at the KSHV-infected BC-3 or BC-1 cells membrane prior to secretion. An investigation of the antigenic specificities of MAbs against KSHV vMIP-I and vMIP-II in MCD and KS patients has not yet been reported. Here, immunohistochemical analysis detected only vMIP-II in samples from both KS and MCD patients, but vMIP-I was not detected in KS cases: however, both vMIP-I and vMIP-II proteins were expressed in some cells in the interfollicular zone of MCD tissues. Lytic proteins of the KSHV such as K8, RTA, and ORF59 have been detected in large lymphocytes in the mantle zone of MCD cases (Dupin et al., 1999; Katano et al., 2000a). The expression of vMIPs showed a similar pattern to that of the lytic proteins in MCD tissues. In contrast, lytic protein expression, including that of vMIPs, was rare in the KS lesions (Abe et al., 2006). In the present study, we demonstrated that vMIPs were expressed in the cells expressing ORF59 protein. Thus, our data clearly indicated that the expression of vMIPs is associated with lytic infection in individual cells affected by KSHV-associated diseases. Human monocytic cell line THP-1 respond to various chemokines suggesting that they express receptors for these chemokines (Wang et al., 1993). Previous study, vMIP-I and vMIP-II were shown chemotaxis in THP-1 cells (Nakano et al., 2003). It has been reported that vMIP-I acts as a specific agonist for CC chemokine receptor 8 (CCR8) (Dairaghi et al., 1999; Endres et al., 1999) and vMIP-II shows a Ca^{2+} flux as a specific agonist for CCR3 (Boshoff et al., 1997). Our data showed anti-vMIP-I and anti-vMIP-II MAbs were able to neutralize vMIP-I- and vMIP-II-mediated chemotaxis in THP-1 cells. However, neutralizing activities

of anti-vMIP-I MAb was apparently low, even the addition of 10 μg/ml MAbs. These findings support the assumption that anti-vMIP-I and –vMIP-II MAbs-blocked chemotaxis in THP-1 cells act through binding to the certain amino acid residue of vMIP-I and vMIP-II.

In summary, MAbs developed specifically for this series were used to detect vMIP-I and vMIP-II in MCD and KS tissues, which may account for certain clinical features of MCD and KS. To gain a better understanding of these important viral genes, additional studies will be needed that focus on revealing vMIP-I and vMIP-II expression profiles during lytic infection. Taken together, these studies provide an insight into the pathogenesis of the contribution of vMIP-I and vMIP-II to the lytic induction of KSHV. These MAbs could serve as useful tools to clarify the pathogenesis of KSHV-related diseases.

Acknowledgments

This study was supported by a grant for Research on Publicly Essential Drugs and Medical Devices from the Japan Health Sciences Foundation (SAA4832), Health and Labor Sciences Research Grants (to HK, No. H23-AIDS-Ippan-002) from the Ministry of Health and by a grant from PRESTO of the Japan Science and Technology Corporation (200154023).

References

Abe, Y., Matsubara, D., Gatanaga, H., Oka, S., Kimura, S., Sasao, Y., Saitoh, K., Fujii, T., Sato, Y., Sata, T., Katano, H., 2006. Distinct expression of Kaposi's sarcoma-associated herpesvirus-encoded proteins in Kaposi's sarcoma and multicentric Castleman's disease. Pathol. Int. 56, 617–624.

Arvanitakis, L., Mesri, E.A., Nador, R.G., Said, J.W., Asch, A.S., Knowles, D.M., Cesarman, E., 1996. Establishment and characterization of a primary effusion (body cavity-based) lymphoma cell line (BC-3) harboring kaposi's sarcoma-associated herpesvirus (KSHV/HHV-8) in the absence of Epstein-Barr virus. Blood 88, 2648–2654.

Benelli, R., Barbero, A., Buffa, A., Aluigi, M.G., Masiello, L., Morbidelli, L., Ziche, M., Albini, A., Noonan, D., 2000. Distinct chemotactic and angiogenic activities of peptides derived from Kaposi's sarcoma virus encoded chemokines. Int. J. Oncol. 17, 75–81.

Boshoff, C., Endo, Y., Collins, P.D., Takeuchi, Y., Reeves, J.D., Schweickart, V.L., Siani, M.A., Sasaki, T., Williams, T.J., Gray, P.W., Moore, P.S., Chang, Y., Weiss, R.A., 1997. Angiogenic and HIV-inhibitory functions of KSHV-encoded chemokines. Science 278, 290–294.

Cesarman, E., Chang, Y., Moore, P.S., Said, J.W., Knowles, D.M., 1995. Kaposi's sarcoma-associated herpesvirus-like DNA sequences in AIDS-related body-cavity-based lymphomas. N. Engl. J. Med. 332, 1186–1191.

Chang, Y., Cesarman, E., Pessin, M.S., Lee, F., Culpepper, J., Knowles, D.M., Moore, P.S., 1994. Identification of herpesvirus-like DNA sequences in AIDS-associated Kaposi's sarcoma. Science 266, 1865–1869.

Chen, S., Bacon, K.B., Li, L., Garcia, G.E., Xia, Y., Lo, D., Thompson, D.A., Siani, M.A., Yamamoto, T., Harrison, J.K., Feng, L., 1998. In vivo inhibition of CC and CX3C chemokine-induced leukocyte infiltration and attenuation of glomerulonephritis in Wistar–Kyoto (WKY) rats by vMIP-II. J. Exp. Med. 188, 193–198.

Dairaghi, D.J., Fan, R.A., McMaster, B.E., Hanley, M.R., Schall, T.J., 1999. HHV8-encoded vMIP-I selectively engages chemokine receptor CCR8. Agonist and antagonist profiles of viral chemokines. Biol. Chem. 274, 21569–21574.

Dupin, N., Fisher, C., Kellam, P., Ariad, S., Tulliez, M., Franck, N., van Marck, E., Salmon, D., Gorin, I., Escande, J.P., Weiss, R.A., Alitalo, K., Boshoff, C., 1999. Distribution of human herpesvirus-8 latently infected cells in Kaposi's sarcoma, multicentric Castleman's disease, and primary effusion lymphoma. Proc. Natl. Acad. Sci. U. S. A. 96, 4546–4551.

Endres, M.J., Garlisi, C.G., Xiao, H., Shan, L., Hedrick, J.A., 1999. The Kaposi's sarcoma-related herpesvirus (KSHV)-encoded chemokine vMIP-I is a specific agonist for the CC chemokine receptor (CCR)8. J. Exp. Med. 189, 1993–1998.

Katano, H., Sato, Y., Kurata, T., Mori, S., Sata, T., 2000a. Expression and localization of human herpesvirus 8-encoded proteins in primary effusion lymphoma, Kaposi's sarcoma, and multicentric Castleman's disease. Virology 269, 335–344.

Katano, H., Suda, T., Morishita, Y., Yamamoto, K., Hoshino, Y., Nakamura, K., Tachikawa, N., Sata, T., Hamaguchi, H., Iwamoto, A., Mori, S., 2000b. Human herpesvirus 8-associated solid lymphomas that occur in AIDS patients take anaplastic large cell morphology. Mod. Pathol. 13, 77–85.

Kledal, T.N., Rosenkilde, M.M., Coulin, F., Simmons, G., Johnsen, A.H., Alouani, S., Power, C.A., Luttichau, H.R., Gerstoft, J., Clapham, P.R., Clark-Lewis, I., Wells, T.N., Schwartz, T.W., 1997. A broad-spectrum chemokine antagonist encoded by Kaposi's sarcoma-associated herpesvirus. Science 277, 1656–1659.

Miller, G., Heston, L., Grogan, E., Gradoville, L., Rigsby, M., Sun, R., Shedd, D., Kushnaryov, V.M., Grossberg, S., Chang, Y., 1997. Selective switch between latency and lytic replication of Kaposi's sarcoma herpesvirus and Epstein-Barr virus in dually infected body cavity lymphoma cells. J. Virol. 71, 314–324.

Moore, P.S., Boshoff, C., Weiss, R.A., Chang, Y., 1996. Molecular mimicry of human cytokine and cytokine response pathway genes by KSHV. Science 274, 1739–1744.

Nakano, K., Isegawa, Y., Zou, P., Tadagaki, K., Inagi, R., Yamanishi, K., 2003. Kaposi's sarcoma-associated herpesvirus (KSHV)-encoded vMIP-I and vMIP-II induce signal transduction and chemotaxis in monocytic cells. Arch. Virol. 148, 871–890.

Niwa, H., Yamamura, K., Miyazaki, J., 1991. Efficient selection for high-expression transfectants with a novel eukaryotic vector. Gene 108, 193–199.

Schalling, M., Ekman, M., Kaaya, E.E., Linde, A., Biberfeld, P., 1995. A role for a new herpes virus (KSHV) in different forms of Kaposi's sarcoma. Nat. Med. 1, 707–708.

Soulier, J., Grollet, L., Oksenhendler, E., Cacoub, P., Cazals-Hatem, D., Babinet, P., d'Agay, M.F., Clauvel, J.P., Raphael, M., Degos, L., et al., 1995. Kaposi's sarcoma-associated herpesvirus-like DNA sequences in multicentric Castleman's disease. Blood 86, 1276–1280.

Sun, R., Lin, S.F., Staskus, K., Gradoville, L., Grogan, E., Haase, A., Miller, G., 1999. Kinetics of Kaposi's sarcoma-associated herpesvirus gene expression. J. Virol. 73, 2232–2242.

Wang, J.M., McVicar, D.W., Oppenheim, J.J., Kelvin, D.J., 1993. Identification of RANTES receptor on human monocytic cells: competition of binding and desensitization by homologous chemotactic cytokines. J. Exp. Med. 177, 699–705.

Pediatric Dermatology Vol. 28 No. 1 23–25, 2011

A Case of Erythema Multiforme Associated with Primary Epstein–Barr Virus Infection

Hidetaka Nakai, M.D.,* Ken Sugata, M.D.,* Chie Usui, M.D.,* Yoshizo Asano, M.D.,* Takashi Yamakita, M.D.,† Kayoko Matsunaga, M.D.,† Yoshikazu Mizokuchi, M.D.,‡ Harutaka Katano, D.D.S.,§ Keiji Iwatsuki, M.D.,¶ and Tetsushi Yoshikawa, M.D.*

**Department of Pediatrics, Fujita Health University School of Medicine, Aichi, †Department of Dermatology, Fujita Health University School of Medicine, Aichi, ‡Department of Pathology, Fujita Health University School of Medicine, Aichi, §Department of Pathology, National Institute of Infectious Diseases, Shinjuku, Tokyo, ¶Department of Dermatology, Okayama University Graduate School of Medicine and Dentistry, Okayama, Okayama, Japan*

Abstract: **We present a case of primary Epstein–Barr virus (EBV) infection with erythema multiforme. A 1-year-old Japanese boy presented with skin eruptions, including typical target lesions and a low-grade fever. Just before the skin biopsy, 95 copies/μg DNA of EBV genome was detected in peripheral blood mononuclear cells, which subsequently increased to 6,834 copies/μg DNA. Skin tissue collected from the skin lesion showed the typical pathologic findings of erythema multiforme. EBV-encoded small nuclear RNA signals were not detected in the skin tissue by *in situ* hybridization.**

Primary Epstein–Barr virus (EBV) infection can produce several cutaneous findings. Although a strong correlation was found between EBV infection and drug eruptions, particularly ampicillin-associated drug eruption, EBV infection with erythema multiforme is rare. Only two case reports in the English scientific literature have described infectious mononucleosis patients with erythema multiforme (1,2). However, one case reported lacked virologic examinations (1), and neither was analyzed with *in situ* hybridization to determine if EBV was present in skin tissue. We report a case of primary EBV infection with erythema multiforme, in which we performed virologic examinations, including *in situ* hybridization and real-time polymerase chain reaction (PCR), to elucidate the pathogenesis of EBV-associated erythema multiforme.

CASE REPORT

A 1-year-old Japanese boy presented with a 3-day history of skin eruptions and a low-grade fever. Skin lesions started on his face, and then expanded to his trunk and extremities. One day before visiting our hospital, he was prescribed steroid ointment by a general practitioner. He had no pre-existing skin diseases and no history of prior medications except for the ointment. During his first examination at our outpatient clinic, he had an erythematous macular skin rash including typical target

Address correspondence to Tetsushi Yoshikawa, M.D., Department of Pediatrics, Fujita Health University School of Medicine, Toyoake 4701192, Japan, or e-mail: tetsushi@fujita-hu.ac.jp.

DOI: 10.1111/j.1525-1470.2010.01217.x

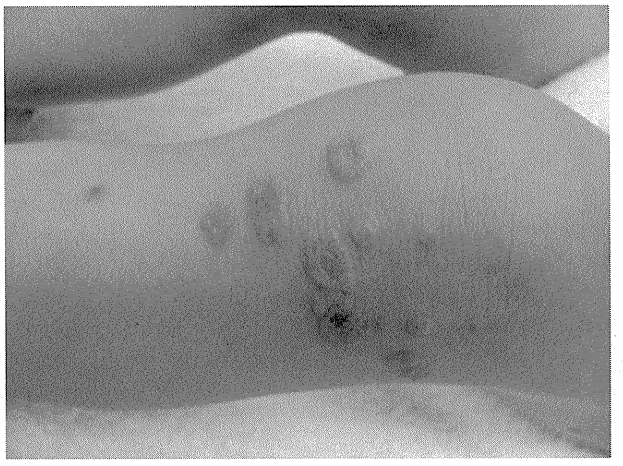

Figure 1. Typical target lesions of erythema multiforme on the lower extremity.

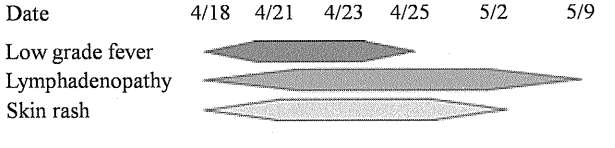

WBC (/μl)	18200	18300		11400
CRP (mg/dl)	<0.3	<0.3		<0.3
Atypical lymphocytes (%)		1		1
EBV VCA IgG		320		320
EBV VCA IgM		80		10
EBV EADR IgG		20		20
EBV EBNA		<10		<10
EBV DNA (copies/μg DNA)		94.8		6834.1

Figure 2. The time course of the patient's laboratory findings and clinical features is shown. The copy numbers of Epstein–Barr virus (EBV) DNA in peripheral blood mononuclear cells were measured using real-time polymerase chain reaction (PCR) method.

lesions on the cheeks, shoulders, and upper and lower extremities (Fig. 1). He had pharyngeal erythema, mild cervical lymphadenopathy but no stomatitis, tonsillitis, or hepatosplenomegaly. Hematologic examinations showed leukocytosis (WBC: 18200/mm^3) with 1% atypical lymphocytes. Hepatic transaminase levels were normal. Serologic examinations showed a typical pattern of primary EBV infection as shown in the Fig. 2 and neither *Mycoplasma pneumoniae* nor herpes simplex virus (HSV) infection was detected by serologic assays. Two days later, because of increasing skin lesions a skin biopsy was performed. Findings included a mononuclear cell infiltration in the upper dermis and inter-cellular edema in the subepidermis (Fig. 3), consistent with erythema multiforme. His symptoms gradually improved without specific treatment and resolved completely in 2 weeks.

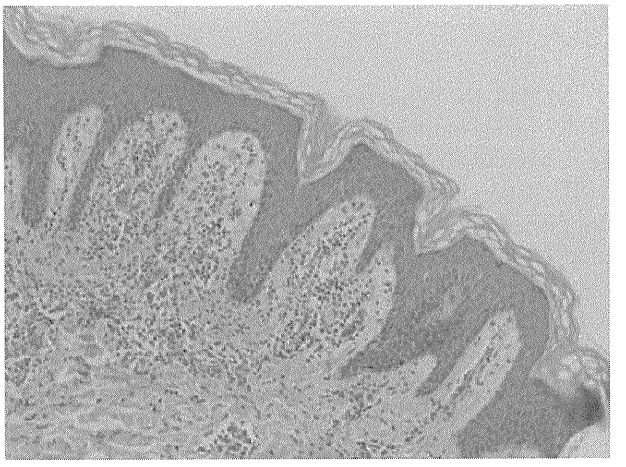

Figure 3. The skin tissue showed mononuclear cell infiltration in the upper dermis and inter-cellular edema in the subepidermis.

To determine whether the disease was cause by EBV, the EBV DNA load in peripheral blood mononuclear cells was measured using real-time PCR. Additionally, an *in situ* hybridization analysis was also performed to detect EBV-encoded small nuclear RNA (EBER) signals in the skin tissue. At his second visit, the day of skin biopsy, 95 copies/μg DNA of EBV genome were detected in the peripheral blood mononuclear cells, and this subsequently increased to 6,834 copies/μg DNA 2 weeks later. No EBER signal was detected in the initial skin tissue biopsy.

DISCUSSION

Erythema multiforme is caused by several stimuli including drugs, viruses, and bacteria. Among these etiologic agents, HSV is the most common cause of the disease; however, the precise mechanism of the disease is still under investigation (3,4). Although two cases of infectious mononucleosis with erythema multiforme have been reported (1,2), only one of these patients was confirmed to have EBV infection by serologic analysis, and no pathologic analysis was performed in either of these two case studies. In the present case, the patient had not been administered any prior medications, and primary EBV infection was confirmed by a serologic assay. In addition, two major etiologic agents, *Mycoplasma pneumoniae* and HSV, were excluded by a serologic analysis. Therefore, we consider that primary EBV infection is the most likely causative agent for erythema multiforme in this patient, and according to the kinetics of EBV DNA load analyzed using real-time PCR, the erythema multiforme occurred early in the course of primary EBV infection in this patient.

As HSV DNA has been detected in the epidermal cells of erythema multiforme lesions, this virus is considered to be a major etiologic agent for the disease (3). Similar to HSV, EBV localization in the skin tissue should be confirmed to elucidate the pathogenesis of EBV-associated erythema multiforme. Although an *in situ* hybridization analysis was performed, no EBER signal was detected in the patient's skin tissue. Chen et al (5) reported that EBV DNA was detectable in two of 32 skin tissues collected from adult patients with erythema multiforme; however, no serologic analysis of EBV infection was performed in these two patients. Although viral DNA was detected in the two samples, EBER was not detected in the skin tissues, similar to this study. This previous study (5) in addition to the present case report suggests that active EBV infection does not occur in the epidermal cells of EBV-associated erythema multiforme. As only a small amount of EBV DNA (95 copies/μg DNA) was contained in peripheral blood mononuclear cells at the time of skin biopsy, the signal *in situ* hybridization from the infiltrated cells may have been below the sensitivity of the assay. Although HSV DNA has been detected in the epidermal cells of erythema multiforme lesions (3), viral replication in the skin appears to be limited because viral particles are not detected in skin tissue (6). Therefore, more in-depth virologic analyses that detect either viral antigens or other types of viral RNA are required to elucidate the pathogenesis of EBV-associated erythema multiforme.

To our knowledge, this is the first report of EBV-associated erythema multiforme analyzed by *in situ* hybridization. This patient lacked the typical clinical symptoms of infectious mononucleosis except for leukocytosis and mild lymphadenopathy. Therefore, EBV should be regarded as a potential cause of erythema multiforme, even though the patient lacked symptoms of infectious mononucleosis.

REFERENCES

1. Williamson DM. Erythema multiforme in infectious mononucleosis. Br J Dermatol 1974;91:345–346.
2. Hughes J, Burrows NP. Infectious mononucleosis presenting as erythema multiforme. Clin Exp Dermatol 1993;18:373–374.
3. Brice SL, Krzemien D, Weston WL et al. Detection of herpes simplex virus DNA in cutaneous lesions of erythema multiforme. J Invest Dermatol 1989;93:183–187.
4. Aurelian L, Ono F, Burnett J. Herpes simplex virus (HSV)-associated erythema multiforme (HAEM): a viral disease with an autoimmune component. Dermatol Online J 2003;9:1.
5. Chen CL, Chow KC, Wong CK et al. A study on Epstein-Barr virus in erythema multiforme. Arch Dermatol Res 1998;290:446–449.
6. Aurelian L, Kokuba H, Burnett JW. Understanding the pathogenesis of HSV-associated erythema multiforme. Dermatology 1998;197:219–222.

frontiers in
MICROBIOLOGY

REVIEW ARTICLE
published: 25 August 2011
doi: 10.3389/fmicb.2011.00175

Pathology of Kaposi's sarcoma-associated herpesvirus infection

*Hitomi Fukumoto[1,2], Takayuki Kanno[1], Hideki Hasegawa[1] and Harutaka Katano[1]**

[1] *Department of Pathology, National Institute of Infectious Diseases, Tokyo, Japan*
[2] *Military Medicine Research Unit, Japan Ground Self Defense Force, Tokyo, Japan*

Edited by:
Keiji Ueda, Osaka University Graduate School of Medicine, Japan

Reviewed by:
Hiroki Isomura, Aichi Cancer Center Research Institute, Japan
Keiji Ueda, Osaka University Graduate School of Medicine, Japan

****Correspondence:***
Harutaka Katano, Department of Pathology, National Institute of Infectious Diseases, 1-23-1 Toyama, Shinjuku-ku, Tokyo 162-8640, Japan.
e-mail: katano@nih.go.jp

Kaposi's sarcoma-associated herpesvirus (KSHV; human herpesvirus 8) is a human herpesvirus, classified as a gamma-herpesvirus. KSHV is detected in Kaposi's sarcoma (KS), primary effusion lymphoma (PEL), and some cases of multicentric Castleman's disease (MCD). Similar to other herpes viruses, there are two phases of infection, latent and lytic. In KSHV-associated malignancies such as KS and PEL, KSHV latently infects almost all tumor cells. Quantitative PCR analysis revealed that each tumor cell contains one copy of KSHV in KS lesions. The oncogenesis by KSHV has remained unclear. Latency-associated nuclear antigen (LANA)-1 plays an important role in the pathogenesis of KSHV-associated malignancies through inhibition of apoptosis and maintenance of latency. Because all KSHV-infected cells express LANA-1, LANA-1 immunohistochemistry is a useful tool for diagnosis of KSHV infection. KSHV encodes some homologs of cellular proteins including cell-cycle regulators, cytokines, and chemokines, such as cyclin D, G-protein-coupled protein, interleukin-6, and macrophage inflammatory protein-1 and -2. These viral proteins mimic or disrupt host cytokine signals, resulting in microenvironments amenable to tumor growth. Lytic infection is frequently seen in MCD tissues, suggesting a different pathogenesis from KS and lymphoma.

Keywords: Kaposi's sarcoma-associated herpesvirus, HHV-8, latency-associated nuclear antigen, LANA-1, primary effusion lymphoma

INTRODUCTION

The 1994 discovery of Kaposi's sarcoma-associated herpesvirus (KSHV, human herpesvirus 8, HHV-8) in Kaposi's sarcoma (KS) tissues had a huge impact, not only in the field of virology, but also on bioscience generally (Chang et al., 1994; Ganem, 2005). Before the discovery of KSHV, almost all viruses had been identified using conventional virus isolation methods with cell cultures. DNA fragments of KSHV were identified in KS tissues by representational difference analysis, which is a subtraction PCR-based method to purify restriction-endonuclease-digested fragments present in one population of DNA fragments but not in others (Chang et al., 1994). Thus, KSHV is the first virus whose fragments were identified directly by the PCR method before any cell culture methods. In 1996, KSHV-infected cell lines were established, based on the fragments' DNA sequences (Renne et al., 1996b). Herpesvirus-like particles of this virus were found in lymphoma cells by electron microscopic analysis. Finally, KSHV's full DNA sequence was determined (Russo et al., 1996). Over the 15-years since the discovery of KSHV, it has been established as a tumor virus (Ganem, 2005). Some KSHV-encoded genes are homologous to oncogenes or cell-cycle-associated genes (Russo et al., 1996); some are transformational genes, able to transform human cells (Gao et al., 1997; Bais et al., 1998; Lee et al., 1998; Muralidhar et al., 1998). However, expression of KSHV-encoded genes is severely restricted; only a few viral genes are expressed in KSHV-infected cells. The KSHV-encoded latency-associated nuclear antigen 1 (LANA-1) is the only protein whose expression is stably detected by immunohistochemistry in KSHV-infected cells (Dupin et al., 1999; Katano et al., 2000b). LANA-1 is a multifunctional protein, but has no full transforming activity. In comparison, Epstein–Barr virus (EBV) encodes a full oncogenic protein, latent membrane protein-1 (LMP1), which is expressed in a subset of EBV-latently infected cells (Cohen, 2000). Thus, KSHV oncogenesis is not simple. Many KSHV-encoded non-transforming proteins apparently collaborate to establish and maintain oncogenesis in KSHV-infected cells. In this review, the pathological aspects of KSHV infection and KSHV-associated diseases are summarized.

VIRUS AND ITS GENE EXPRESSION

Usually, viral particles are not observed in KS samples by electron microscope because of the small number of KSHV copies. However, they can be seen in primary effusion lymphoma (PEL) cell lines stimulated by 12-*O*-tetradecanoylphorbol-13-acetate (TPA). A complete viral particle of KSHV, consisting of a capsid and an envelope (Renne et al., 1996b; Said et al., 1996, 1997; Orenstein et al., 1997; Ohtsuki et al., 1999), is 150–200 nm in diameter, which is similar to other human herpes viruses and indistinguishable from other herpes viruses. The unenveloped capsid is produced in the host nucleus and is 100 nm in diameter. It contains a central DNA core, which appears to have a high electron density. The envelope is derived from the inner nuclear membrane, as viral particles bud into the cytoplasm from the nucleus. The tegument protein fills the space between the nucleocapsid and envelope. This feature

of viral particles is apparently quite similar among herpes viruses, but related structures forming in infected cells seem to depend on the type of virus.

The KSHV genome consists of linear, double-stranded DNA of about 170 kbp (Renne et al., 1996a; Russo et al., 1996). The KSHV genome consists of a long unique region (LUR) and a terminal repeat (TR) at both termini, which resembles the herpes virus saimiri structure (Russo et al., 1996). The TRs consist of 801-bp direct repeat units having 84.5% GC content. The number of repeats in TRs may vary. The LUR is 140.5 kbp and has 53.5% GC content. KSHV encodes more than 80 viral proteins on LUR. KSHV also encodes 17 microRNAs (miRNAs), which are derived by processing from 12 pre-miRNAs (Cai et al., 2005). Kinetics of KSHV-encoded genes were mainly investigated in KSHV-infected PEL cell lines stimulated with phorbol ester such as TPA (Sun et al., 1999). Like other herpesviruses, viral genes were categorized into lytic and latent genes, and also into immediate-early (IE), early (E), and late (L) genes based on their expressions. The function of each KSHV-encoded gene was summarized in the **Table 1**. Open reading frame 50 (*ORF50*) is an IE gene that is a homolog of *Rta*, a transcriptional activator encoded by EBV (Lukac et al., 1999; Seaman et al., 1999; Sun et al., 1999; Zhu et al., 1999). Transcription of *ORF50* results in its expression within 4 h after stimulation by TPA. This expression could not be blocked by phosphonoacetic acid (a herpesvirus-DNA polymerase inhibitor) nor cycloheximide (a protein synthesis inhibitor). Transfection of *ORF50* to KSHV-infected cells resulted in the activation of lytic gene expression (Lukac et al., 1999). Thus, ORF50 protein is a lytic switch protein. Expression of ORF50 protein is required for expression of many KSHV-encoded lytic genes such as *K3*, and *K5* (homologs of the IE gene of *BHV-4*), viral interleukin-6 (*vIL-6*), viral macrophage inflammatory proteins (*vMIPs*), polyadenylated nuclear RNA (*PAN*), *vBcl-2*, *K12*, viral G-protein-coupled receptor (*vGPCR*), viral dihydrofolate reductase (*vDHFR*), DNA replication factors, and thymidylate synthase (Sarid et al., 1998). ORF50 protein also induces expression of K8 (K-bZIP, a positional homolog of EBV BZLF1) protein, an early protein. K8 protein plays a role as transactivation repressor for ORF50 protein, leading to a negative autoregulation system during lytic infection (Liao et al., 2003). Late genes, including tegument proteins, and virion-associated protein are then expressed (**Table 1**).

Latent infection is predominant in KSHV infection. KSHV codes a latency-associated gene cluster including *ORF73* (*LANA-1*, *LNA*, or *LNA-1*), v-cyclin (*ORF72*), viral FLICE-inhibitory protein (*K13*, *v-FLIP*), Kaposin (*K12*), and viral-encoded miRNAs. LANA-1 is always detected as a dot-like staining pattern in KSHV-infected cells by immunohistochemistry. KSHV-encoded 17 miRNAs, which are derived by processing from 12 pre-miRNAs, are expressed during viral latency (Cai et al., 2005; Samols et al., 2005).

Table 1 | Kaposi's sarcoma-associated herpesvirus genes and their functions.

Gene	Phase	Functions
LANA-1	Latent	Always express in KSHV-infected cells Maintain and replicate viral genome during mitotic division by holding KSHV episome at chromosome Bind to p53 and inhibit p53-dependent apoptosis Bind to Rb and inhibit Rb-E2F pathway Bind to GSK-3β, and induce accumulation of β-catenin
LANA-2	Latent	Expressed in only PEL cells, not in KS cells Homolog of IRF Inhibit p53-dependent apoptosis
Kaposin	Latent	Kaposin A: transformation activity? Kaposin B, C: associate with cytokine expression as adaptor protein of MAP kinase-associated protein kinase 2 (MK2)
v-cyclin	Latent	Homolog of cyclin D1 Inhibit P27Kip1, and induce cell-cycle to S-phase
v-FLIP	Latent	Anti-apoptosis
ORF50 (RTA)	Lytic (IE)	Lytic switch protein Transactivator for K8
K1	Lytic	Transformation activity
K8	Lytic (early)	Transcriptional repressor for RTA
K3, K5	Lytic (IE/early)	Down-regulation of MHC class I expression
vIL-6	Lytic (early)	Induce VEGF expression Induce constitutional activation of Stat3 Disrupt anti-viral function by IFN-α
vIRF-1	Lytic (early)	Disrupt IFN signal Transformation activity?
vMIPs	Lytic (early)	Bind to chemokine receptors and induce angiogenesis
vBcl-2	Lytic (early)	Inhibit apoptosis
vGPCR	Lytic (early)	Transformation activity Bind to IL-8 Induce VEGF expression
K15	Lytic	Bind to TRAF family, and induction of NF-κB activation

KSHV ONCOGENESIS

The first evidence of transformation activity by KSHV came from a report describing that human umbilical vein endothelial cells (HUVEC) were transformed and immortalized by KSHV infection *in vitro* (Flore et al., 1998). However, such KSHV-infected HUVEC did not express any KSHV gene, and the immortalization by KSHV infection was not confirmed by any other groups (Gao et al., 2003; Tang et al., 2003). KSHV efficiently infects primary cultures of human endothelial cells *in vitro* (Sakurada et al., 2001; Gao et al., 2003). KSHV-infected cells express LANA-1 within several hours after infection. One week after infection, a large portion of culture cells will be infected by KSHV and expressing LANA-1. Interestingly, expression of any lytic proteins encoded by KSHV is not observed at that time. Latent infection is dominant in KSHV-infected cells *in vivo* and *in vitro*. Although some KSHV-encoded proteins such as K1 and vGPCR

are shown to have a transformation activity on mammalian cells, these transforming proteins are not usually expressed in KSHV-infected cells (Bais et al., 1998; Lee et al., 1998; Montaner et al., 2003). However, LANA-1, a major KSHV-encoded latency protein, is always expressed in KSHV-infected cells both *in vivo* and *in vitro* (Dupin et al., 1999; Katano et al., 1999b; Kellam et al., 1999). Moreover, latency is maintained during the presence of KSHV in the cells. Thus, LANA-1 clearly plays an important role in the pathogenesis of KSHV infection, and has been shown to be a multifunctional protein. Probably the most important role of LANA-1 is to establish and maintain the latency in KSHV-infected cells by tethering KSHV DNA to host chromosomes (Ballestas et al., 1999). LANA-1 binds directly to TR sequences of the KSHV genome, and recruits it to the host chromosome (**Figure 1E**). The DNA of KSHV is replicated during host cell divisions using host DNA replicative machinery (Sakakibara et al., 2004). Thus, daughter cells inherit KSHV genome without any virus particle. LANA-1 is also associated with signal transduction in KSHV-infected cells. LANA-1 binds directly to p53, a major tumor repressor and anti-apoptotic factor (Friborg et al., 1999). Viral infection usually induces p53 expression and p53-dependent apoptosis as self-defense system. Direct interaction with p53 by LANA-1 results in inhibition of p53-dependent apoptosis in KSHV-infected cells. Moreover, LANA-1 stabilizes β-catenin by binding to the negative regulator GSK-3β, promoting cell-cycle induction by nuclear accumulation of GSK-3β (Fujimuro et al., 2003). Thus, LANA-1 plays a central role in the pathogenesis of KSHV infection, but LANA-1 itself does not have any full transformation activity. Many other factors besides LANA-1 are required to establish KSHV oncogenesis.

Another important factor in KSHV oncogenesis is that KSHV encodes many homologs of human genes. The viral genes of human gene homologs cooperate to establish suitable growth conditions for KSHV-infected cells. Among them, vIL-6 is the most important factor for KSHV pathogenesis. vIL-6 induces angiogenesis by vascular endothelial cell growth factor (VEGF) expression (Aoki et al., 1999), and stimulates the constitutive Jak-Stat pathway through the Stat3 signal, resulting in cell growth (Aoki et al., 2003). In addition, vIL-6 represses the anti-viral function of interferon by binding to a subunit of human IL-6 receptor and suppressing p21 expression (Chatterjee et al., 2002). KSHV-encoded vMIP-1, vMIP-2, vBcl-2, vIRF-1, v-cyclin D, and v-FLIP mimic their human homologs, and work sometimes as inhibitors and sometimes as mimics, resulting in growth of KSHV-infected cells. Because almost all these mimics are lytic proteins, their expression is not usually observed. However, some cytokines may induce their expression independently to lytic and latent infection as necessary. Thus, KSHV oncogenesis is established by cooperation of many viral proteins such as LANA-1 and by the mimic, rather than the primary functions of oncogenetic transformation genes encoded by the virus.

Recently, miRNA has been shown to affect tumor biology. Several KSHV miRNAs were shown to modulate host gene expression, suggesting some roles for miRNA in the pathogenesis of KSHV-induced malignancies. Thrombospondin 1, a potent inhibitor of angiogenesis that is reportedly downregulated in KS lesions, is targeted by multiple miRNAs (Samols et al., 2007). The target of miR-K5 is Bcl2-associated factor BCLAF1, which promote apoptosis (Lei et al., 2010). MiR-K1 targets IκBα, an inhibitor of NF-κB. NF-κB inhibits the activation of lytic viral promoters. By activating NF-κB, miR-K1 suppresses viral lytic replication, maintaining latent infection (Ziegelbauer et al., 2009). So far, miRNAs' roles in viral infection and replication remain unclear.

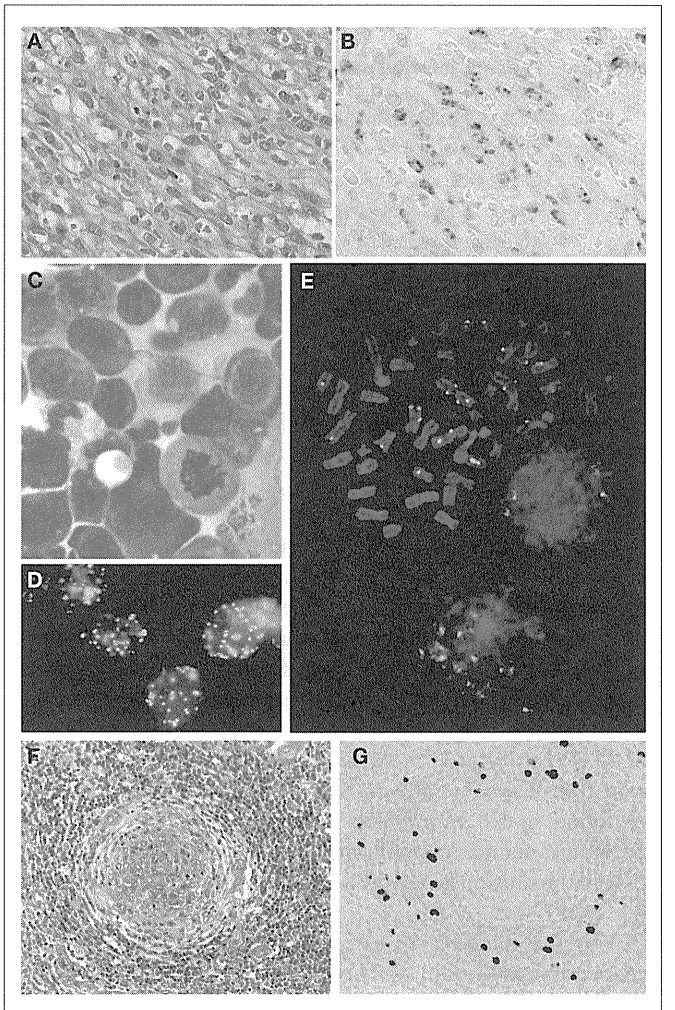

FIGURE 1 | Histological analysis on KSHV-associated diseases. (A) Nodular stage of KS; HE staining. **(B)** LANA-1 immunohistochemistry of KS. **(C)** Giemsa staining of PEL. **(D)** LANA-1 immunofluorescence staining in mitosis of PEL cells. **(E)** LANA-1 immunostaining of mitosis of PEL cell line, TY-1. Yellow signals indicate LANA-1. Red is counter staining of chromosome. **(F)** HE staining of MCD. **(G)** LANA-1 immunohistochemistry of MCD.

EPIDEMIOLOGY

Serological studies have revealed that KSHV-infected individuals are found all over the world. Serum antibody to KSHV is detected with ELISA using lysate of KSHV viral particles or recombinant viral proteins as antigens, or immunofluorescence assay using KSHV-infected cells. The seroprevalence of KSHV infection differs among regions/countries. Among the general population, KSHV seropositivity is less than 10% in northern Europe, America, and Asia, 10–30% in the Mediterranean region, and more than

Table 2 | Kaposi's sarcoma-associated herpesvirus genotypes.

Genotype	Patients, infected persons
A	AIDS–KS patients in the US, Europe, Eurasia
B	KS patients of African heritage
C	Classic KS, iatrogenic, and AIDS–KS in Eurasia, US AIDS–KS, Taiwan, Korea, China, Middle East
D	KS patients of Pacific island
E	South American (partial), Brazil Amerindian, Guinea Amerindian

50% in most of sub-Saharan Africa (Davis et al., 1997; Kedes et al., 1997; Chatlynne et al., 1998; Mayama et al., 1998; Rabkin et al., 1998; Katano et al., 2000a). The homosexual population exhibits higher positivity (8–25%) than the general population (Grulich et al., 2005; Casper et al., 2006; Engels et al., 2007). Although the transmission modes of KSHV have not yet been clarified, transmission though saliva is likely (Pauk et al., 2000), because high KSHV copy numbers are detected in saliva of seropositives. Horizontal transmission through the saliva transmission is suggested among children in endemic countries, while sexual transmission may be predominant among homosexual men in non-endemic countries. Organ transplantation can transmit KSHV (Regamey et al., 1998). Transmission of KSHV through blood transfusion is controversial. While KSHV seroconversion was found in US transfusion recipients (Hladik et al., 2006), later studies found no significant association of KSHV infection between transfusion groups and non-transfusion groups (Cannon et al., 2009).

Genotypes of KSHV are categorized based on sequences of the hypervariable regions in its *K1* gene (Meng et al., 1999; Zong et al., 1999; Biggar et al., 2000; Kazanji et al., 2005; Hayward and Zong, 2007; Kanno et al., 2010). The KSHV *K1* genes are classified into at five groups: A, B, C, D, and E (**Table 2**). Geographical differences in KSHV genotypes may reflect the history of migration of human populations (Zong et al., 1999). Subtypes A and C were detected in Japan and subtype A was seen more frequently in AIDS-associated cases than non-AIDS patients (Kanno et al., 2010). There is no correlation between genotype and KSHV-related disease, including KS, PEL, and multicentric Castleman's disease (MCD).

KSHV-RELATED DISEASES

Fragments of the KSHV genome have been detected in DNA samples extracted from various diseases by PCR. However, the only diseases whose associations with KSHV infection are widely accepted among researchers in this field are KS, PEL, and MCD (**Table 3**). KSHV is distributed all over the world, and there are many individuals with KSHV infections. Therefore, a low KSHV titer, as detected by PCR, does not mean that a disease is associated with KSHV infection. Because KSHV LANA-1 is always expressed in KSHV-infected cells, LANA-1 immunohistochemistry is a powerful and confirmative tool to detect KSHV-infected cells in pathological samples, and the association with KSHV infection in diseases should be examined by LANA-1 immunohistochemistry on tissue samples.

Table 3 | Kaposi's sarcoma-associated herpesvirus and diseases.

Usually detected (Confirmed association in all cases)	Kaposi's sarcoma (all subtypes), primary effusion lymphoma
Partially detected (Confirmed association only in KSHV$^+$ cases)	Multicentric Castleman's disease including POEMS (polyneuropathy, organomegaly, endocrinopathy, M protein, skin changes) syndrome, febrile maculopapular skin rash, hemophagocytic syndrome
Detected in reports, but no association with KSHV infection	Multiple myeloma, primary pulmonary hypertension, Bowen disease, squamous cell carcinoma, Paget disease, actinic keratosis etc.

PRIMARY KSHV INFECTION

A mass study of immunocompetent children in Egypt, where KSHV infection is common, suggested that a febrile maculopapular skin rash was associated with primary KSHV infection (Andreoni et al., 2002). Seroconversion for KSHV was confirmed in those patients and transmission through saliva was implied by DNA sequences in saliva. A study of homosexual men without HIV infection suggested that diarrhea, fatigue, localized skin rash, and lymphadenopathy were also symptoms of primary KSHV infection (Wang et al., 2001). Moreover, active KSHV infection may be associated with non-malignant illnesses such as fever, cutaneous rash, and hepatitis after peripheral blood stem cell/bone marrow transplantation (Luppi et al., 2000).

KAPOSI'S SARCOMA

Kaposi's sarcoma is most important and common of KSHV-associated diseases. Four clinical subtypes have been recognized: classic, AIDS-associated, post-transplantational (iatrogenic or immunodeficient), and African (endemic) subtypes (Antman and Chang, 2000). These four subtypes of KS are histologically indistinguishable. In the AIDS–KS subtype, KS occurs only in homosexual men. KS occurs in the skin, oral cavity, gastrointestinal tract, lung, liver, lymph node, etc. Skin lesions of KS are most common; they are clinically classified as patchy, plaque, and nodular stages. In the patchy stage, small red flat lesions are observed on the skin. Histologically, dilated, abnormally shaped blood vessels with extravasated red blood cells and edema are found in KS lesions. In the plaque stage, patchy lesions fuse together to form plaque lesions. Proliferation of the spindle-shaped cells is seen around vessels in the plaque stage. In the final nodular stage, brown nodular, and elevated lesions are observed. Histologically, proliferation of spindle cells with slit-like vascular spaces is found (**Figure 1A**). Multiple KS lesions in the extremities or face are often complicated with lymphedema. Pulmonary lesions may lead to fatal respiratory compromise.

Kaposi's sarcoma should be diagnosed with histology and immunohistochemistry. Immunohistochemical staining with anti-LANA-1 antibody shows that the viral protein is expressed in KS cells, irrespective of clinical type or disease stage (Dupin et al., 1999; Katano et al., 1999b). Expression of LANA-1 can be seen in nuclei of KS spindle cells with a speckled pattern (**Figure 1B**). The

lymphatic marker, podoplanin (D2-40), is also expressed in KS cells (Weninger et al., 1999). In addition to histological investigation, PCR analysis is useful for the KS diagnosis. Because each KS cell contains about one copy of the KSHV genome, KSHV DNA fragments are consistently detected by PCR, even in formalin-fixed paraffin-embedded KS tissues (Asahi-Ozaki et al., 2006). PCR sometimes, but not always, detects KSHV DNA in the sera of KS patients. Serum antibody to KSHV is usually positive in KS patients.

Highly active anti-retroviral therapy (HAART) is effective on KS. Incidence of KS in HIV-infected persons has dramatically decreased in the HAART era. Regression of KS is often observed in patients administrated with HAART. In patients with low CD4 counts, KS progresses earlier than in patients with high CD4 counts. These data suggest that KS progression depends on the host's immune status (Bower et al., 2009). Recently, patients with KS were administrated with HAART. Patients with aggressive KS received a combination therapy of HAART and chemotherapy of pegylated liposomal doxorubicin (Martin-Carbonero et al., 2008). Irradiation or surgical resection is also performed for the case of small skin lesion in addition to HAART. There is no effective anti-KSHV therapy for KS. Although vaccine is the most effective method to prevent viral diseases, no vaccine against KSHV is commercially available at present.

The pathological roles of KSHV in KS have been intensely investigated for a long time. The origin of KS cells is thought to be endothelial cells. However, cellular protein expression in KS cells is very different from those of endothelial cells. Infection by KSHV induces a dynamic alteration of gene expression in endothelial cells (Hong et al., 2004; Wang et al., 2004). Analysis via DNA array revealed that endothelial cells reduce expression of blood vascular genes and induce markers of lymphatic endothelial cells after KSHV infection *in vitro*. Thus, KSHV can affect the expression level of cellular proteins in endothelial cells. LANA-1 is expressed in the nucleus by almost all KS spindle shaped cells (**Figure 1B**), whereas the expression of lytic proteins is limited in KS lesions. Therefore, it is likely that latent infection by KSHV is important for the pathogenesis of KS. As described above, LANA-1 plays a central role in the establishment and maintenance of latency. In addition to LANA-1, cytokines are important for KS pathogenesis. Some cytokines have been detected in the sera of KS patients at high levels. It has been demonstrated that bFGF, IL-6, oncostatin M (OSM), and tumor necrosis factor (TNF)-alpha are required for growth of KS cells *in vitro* (Liu et al., 1997; Faris et al., 1998; Murakami-Mori et al., 1998). IL-6 is known to be an important growth factor of KS cells especially *in vitro*. KSHV-encoded vIL-6 interacts with the receptor of human IL-6, mimics its function partially, and contributes to immune escape mechanism by KS cells as described above. KSHV-infected cells have several immune escape mechanisms besides that of vIL-6. K5, a lytic protein of KSHV, down-regulates MHC class I and co-activation molecules, enabling productively infected cells to escape both cytotoxic T cell and NK cell responses (Ishido et al., 2000). In addition, latently infected cells are also resistant to cytotoxic T cell responses owing to reduced levels of MHC class I molecules, impaired antigen processing, and expression of the anti-apoptotic KSHV ORF-K13/viral FLICE-inhibitory protein (v-FLIP; Thome et al., 1997).

PRIMARY EFFUSION LYMPHOMA

Primary effusion lymphoma is a rare disease occurring mainly in immunosuppressed patients, in particular HIV-infected homosexual males (Cesarman et al., 1995; Nador et al., 1996). PEL appears as lymphomatous effusions occurring in the pleural, abdominal, or pericardial effusion in the absence of a contiguous tumor mass. Some patients with PEL secondarily develop solid tumors in adjacent structures such as the pleura; these solid tumors have been termed extracavity PEL (Chadburn et al., 2004). About half of PEL patients have KS. These tumors always carry KSHV and are commonly co-infected by EBV. Histologically, the tumor cells exhibit various appearances, from large immunoblastic or plasmablastic cells to cells with more anaplastic morphology (**Figure 1C**). Nuclei vary from large and round to more irregular in shape, with prominent nucleoli. The cytoplasm can be abundant and is deeply basophilic with vacuoles in occasional cells. Binucleated or multinucleated cells resembling Reed–Sternberg cells can be seen. Mitotic figures are typically numerous. PEL cells are derived from post-germinal center B-cells (Jenner et al., 2003). Their immunophenotypes are undetermined, i.e., CD45 (+), CD138 (+), B-cell markers (−), T cell markers (−); however, their immunoglobulin genes are clonally rearranged and hypermutated. PEL cells contain high copy numbers (about 50 copies/cells) of KSHV DNA (Cesarman et al., 1995; Asahi-Ozaki et al., 2006). PEL cells are sometimes co-infected with EBV, while others are infected only with KSHV. However, expressions of LMPs and EBNAs are suppressed in PEL cells. Several KSHV-infected cell lines have been established from PEL cells (Carbone et al., 2010). A $KSHV^+/EBV^-$ cell line, TY-1, was even established from EBV^+ and $KSHV^+$ PEL cases, suggesting that KSHV plays an essential role in the pathogenesis of PEL (Katano et al., 1999a). Infection by KSHV is predominantly latent in PEL cells, which has made PEL cell lines the most widely studied models for KSHV latency. PEL cells express latent genes coded in the latent cluster in KSHV genome (**Figure 1D**). However, it is not easy to detect latent viral protein expressions other than LANA-1. The expression pattern of KSHV-encoded proteins is almost the same as KS, except that PEL cell express LANA-2 protein (Rivas et al., 2001). Most PEL lines display a very small subpopulation of cells that stain for markers of lytic reactivation such as ORF50, ORF59, and K8.1 (Katano et al., 2000b). Although KSHV-encoded vIL-6 is thought as a lytic protein, vIL-6 is detected more frequently in PEL cells than other lytic proteins. It has been demonstrated that vIL-6 is a multifunctional protein; vIL-6 can bind to IL-6 receptor gp130 in the absence of another subunit of IL-6 receptor, gp80, suggesting vIL-6 can induce cytokine signals in a broader range of cell types (Chatterjee et al., 2002). The signal from gp130 often secretes human IL-6 itself, raising the possibility of an autocrine loop. vIL-6 also induces VEGF expression, resulting in an indirect proliferation effect on PEL cells (Aoki et al., 1999).

MULTICENTRIC CASTLEMAN'S DISEASE

Multicentric Castleman's disease is characterized by plasmacytic lymphoadenopathy with polyclonal hyperimmunoglobulinemia

and high levels of IL-6 in the serum. Histologically, follicular hyperplasia with proliferation of plasma cells and hyaline vascular alterations are observed in the lymph nodes (**Figure 1F**). Two distinct histopathologic subtypes have been reported; the hyaline vascular type (HV type) and the plasma cell type (PC-type). The HV type is characterized by enlarged lymphoid follicles, hyalinized germinal centers within an expanded mantle zone, and a highly vascularized interfollicular area. In contrast, in the PC-type, remarkable infiltration of plasma cells is observed in the interfollicular area. Among these mantle zone cells, there are variable numbers of the larger cells, which are approximately twice the size of mantle zone lymphocytes. These cells are characterized by a moderate amount of amphophilic cytoplasm and a large vesicular nucleus containing one or sometimes two prominent nucleoli. These cells have been called plasmablasts, although they frequently have immunoblastic features (Dupin et al., 2000). The plasmablasts are also found in the interfollicular area of PC-type MCD frequently. In some, but not all cases of MCD, KSHV is detected (Soulier et al., 1995). Using PCR, KSHV is frequently detected in tissues obtained from patients with MCD associated with HIV infection, but is very rare in MCD cases without HIV infection (Suda et al., 2001). KSHV was also detected with high frequency in MCD complicated with polyneuropathy, organomegaly, endocrinopathy, M protein, and skin changes (POEMS) syndrome (Belec et al., 1999). Immunohistochemistry for LANA-1 revealed that KSHV-infected cells are localized in the mantle zone of lymphoid follicles (**Figure 1G**). Besides LANA-1, other KSHV-encoded lytic proteins such as vIL-6, K8, and K8.1 are also detected in these cells, suggesting KSHV$^+$ MCD is associated with KSHV-lytic infection (Dupin et al., 1999; Katano et al., 2000b). The KSHV-encoded vIL-6 plays a role in the proliferation of plasma cells, and is also detected in patients' sera at high levels, suggesting high levels of vIL-6 are associated with MCD pathogenesis (Parravicini et al., 1997). High levels of KSHV DNA are also detected in the serum, which can be a marker of progressive MCD.

LARGE B-CELL LYMPHOMA ARISING IN KSHV-ASSOCIATED MCD

Large B-cell lymphoma arising in KSHV-associated MCD is characterized by a monoclonal proliferation of KSHV-infected lymphoid cells resembling plasmablasts expressing IgM, arising in the setting of MCD (Dupin et al., 2000; Oksenhendler et al., 2002). The small confluent sheets of LANA-1$^+$ plasmablasts are seen in the interfollicular zone of KSHV-associated MCD. This type of lymphoma occurs in the lymph node or spleen with generalized lymphadenitis and/or massive splenomegaly. Plasmablasts show stippled nuclear staining for LANA-1 and cytoplasmic staining for vIL-6, and strongly express cIgM with λ light-chain restriction.

CONCLUSION

Since the discovery of KSHV, 16 years have passed. During the period, some useful diagnostic tools have been developed for pathological examination. Anti-LANA-1 antibody is the most powerful tool for diagnosis of pathological samples of KSHV infection. LANA-1 expression is specific to KSHV infection, because all KSHV-infected cells express LANA-1. Real-time PCR is also a powerful tool for diagnosis. Thus, it is not difficult to diagnose KSHV infection in pathological samples. On the other hand, the pathogenesis, and especially the oncogenesis, of KSHV remain unknown. Although many KSHV-encoded proteins have been characterized and their *in vitro* functions revealed, it is still not clear if KSHV can fully transform or immortalize endothelial cells. It has been shown that LANA-1 plays a central role in KSHV pathogenesis. However, LANA-1 is not enough for KSHV oncogenesis. KSHV-encoded non-transforming proteins may collaborate to establish and maintain appropriate environment for KSHV-infected cells. Further studies should reveal the mechanism of the collaboration by KSHV-encoded proteins.

ACKNOWLEDGMENTS

The authors thank Ms. Yuko Sato for her excellent technical assistance. This study was partly supported by a grant for Research on Publicly Essential Drugs and Medical Devices from the Japan Health Sciences Foundation (to Harutaka Katano and Takayuki Kanno, No. SAA4832); Health and Labor Sciences Research Grants (to Harutaka Katano, No. H21-AIDS-Ippan-006, H22-AIDS-Ippan-002, H23-AIDS-Ippan-002, H21-Shinko-Ippan-009) from the Ministry of Health, Labour and Welfare; and Grants-in-Aid for Scientific Research from the Ministry of Education, Culture, Sports, Science and Technology of Japan (to Harutaka Katano, No. 21590520 and 22390243).

REFERENCES

Andreoni, M., Sarmati, L., Nicastri, E., El Sawaf, G., El Zalabani, M., Uccella, I., Bugarini, R., Parisi, S. G., and Rezza, G. (2002). Primary human herpesvirus 8 infection in immunocompetent children. *JAMA* 287, 1295–1300.

Antman, K., and Chang, Y. (2000). Kaposi's sarcoma. *N. Engl. J. Med.* 342, 1027–1038.

Aoki, Y., Feldman, G. M., and Tosato, G. (2003). Inhibition of STAT3 signaling induces apoptosis and decreases survivin expression in primary effusion lymphoma. *Blood* 101, 1535–1542.

Aoki, Y., Jaffe, E. S., Chang, Y., Jones, K., Teruya-Feldstein, J., Moore, P. S., and Tosato, G. (1999). Angiogenesis and hematopoiesis induced by Kaposi's sarcoma-associated herpesvirus-encoded interleukin-6. *Blood* 93, 4034–4043.

Asahi-Ozaki, Y., Sato, Y., Kanno, T., Sata, T., and Katano, H. (2006). Quantitative analysis of Kaposi sarcoma-associated herpesvirus (KSHV) in KSHV-associated diseases. *J. Infect. Dis.* 193, 773–782.

Bais, C., Santomasso, B., Coso, O., Arvanitakis, L., Raaka, E. G., Gutkind, J. S., Asch, A. S., Cesarman, E., Gershengorn, M. C., and Mesri, E. A. (1998). G-protein-coupled receptor of Kaposi's sarcoma-associated herpesvirus is a viral oncogene and angiogenesis activator. *Nature* 391, 86–89.

Ballestas, M. E., Chatis, P. A., and Kaye, K. M. (1999). Efficient persistence of extrachromosomal KSHV DNA mediated by latency-associated nuclear antigen. *Science* 284, 641–644.

Belec, L., Mohamed, A. S., Authier, F. J., Hallouin, M. C., Soe, A. M., Cotigny, S., Gaulard, P., and Gherardi, R. K. (1999). Human herpesvirus 8 infection in patients with POEMS syndrome-associated multicentric Castleman's disease. *Blood* 93, 3643–3653.

Biggar, R. J., Whitby, D., Marshall, V., Linhares, A. C., and Black, F. (2000). Human herpesvirus 8 in Brazilian Amerindians: a hyperendemic population with a new subtype. *J. Infect. Dis.* 181, 1562–1568.

Bower, M., Weir, J., Francis, N., Newsom-Davis, T., Powles, S., Crook, T., Boffito, M., Gazzard, B., and Nelson, M. (2009). The effect of HAART in 254 consecutive patients with AIDS-related Kaposi's sarcoma. *AIDS* 23, 1701–1706.

Cai, X., Lu, S., Zhang, Z., Gonzalez, C. M., Damania, B., and Cullen, B. R. (2005). Kaposi's sarcoma-associated herpesvirus expresses an array of viral microRNAs in latently infected cells. *Proc. Natl. Acad. Sci. U.S.A.* 102, 5570–5575.

Cannon, M. J., Operskalski, E. A., Mosley, J. W., Radford, K., and

Dollard, S. C. (2009). Lack of evidence for human herpesvirus-8 transmission via blood transfusion in a historical US cohort. *J. Infect. Dis.* 199, 1592–1598.

Carbone, A., Cesarman, E., Gloghini, A., and Drexler, H. G. (2010). Understanding pathogenetic aspects and clinical presentation of primary effusion lymphoma through its derived cell lines. *AIDS* 24, 479–490.

Casper, C., Carrell, D., Miller, K. G., Judson, F. D., Meier, A. S., Pauk, J. S., Morrow, R. A., Corey, L., Wald, A., and Celum, C. (2006). HIV serodiscordant sex partners and the prevalence of human herpesvirus 8 infection among HIV negative men who have sex with men: baseline data from the EXPLORE study. *Sex. Transm. Infect.* 82, 229–235.

Cesarman, E., Chang, Y., Moore, P. S., Said, J. W., and Knowles, D. M. (1995). Kaposi's sarcoma-associated herpesvirus-like DNA sequences in AIDS-related body-cavity-based lymphomas. *N. Engl. J. Med.* 332, 1186–1191.

Chadburn, A., Hyjek, E., Mathew, S., Cesarman, E., Said, J., and Knowles, D. M. (2004). KSHV-positive solid lymphomas represent an extracavitary variant of primary effusion lymphoma. *Am. J. Surg. Pathol.* 28, 1401–1416.

Chang, Y., Cesarman, E., Pessin, M. S., Lee, F., Culpepper, J., Knowles, D. M., and Moore, P. S. (1994). Identification of herpesvirus-like DNA sequences in AIDS-associated Kaposi's sarcoma. *Science* 266, 1865–1869.

Chatlynne, L. G., Lapps, W., Handy, M., Huang, Y. Q., Masood, R., Hamilton, A. S., Said, J. W., Koeffler, H. P., Kaplan, M. H., Friedman-Kien, A., Gill, P. S., Whitman, J. E., and Ablashi, D. V. (1998). Detection and titration of human herpesvirus-8-specific antibodies in sera from blood donors, acquired immunodeficiency syndrome patients, and Kaposi's sarcoma patients using a whole virus enzyme-linked immunosorbent assay. *Blood* 92, 53–58.

Chatterjee, M., Osborne, J., Bestetti, G., Chang, Y., and Moore, P. S. (2002). Viral IL-6-induced cell proliferation and immune evasion of interferon activity. *Science* 298, 1432–1435.

Cohen, J. I. (2000). Epstein-Barr virus infection. *N. Engl. J. Med.* 343, 481–492.

Davis, D. A., Humphrey, R. W., Newcomb, F. M., O'Brien, T. R., Goedert, J. J., Straus, S. E., and Yarchoan, R. (1997). Detection of serum antibodies to a Kaposi's sarcoma-associated herpesvirus-specific peptide. *J. Infect. Dis.* 175, 1071–1079.

Dupin, N., Diss, T. L., Kellam, P., Tulliez, M., Du, M. Q., Sicard, D., Weiss, R. A., Isaacson, P. G., and Boshoff, C. (2000). HHV-8 is associated with a plasmablastic variant of Castleman disease that is linked to HHV-8-positive plasmablastic lymphoma. *Blood* 95, 1406–1412.

Dupin, N., Fisher, C., Kellam, P., Ariad, S., Tulliez, M., Franck, N., Van Marck, E., Salmon, D., Gorin, I., Escande, J. P., Weiss, R. A., Alitalo, K., and Boshoff, C. (1999). Distribution of human herpesvirus-8 latently infected cells in Kaposi's sarcoma, multicentric Castleman's disease, and primary effusion lymphoma. *Proc. Natl. Acad. Sci. U.S.A.* 96, 4546–4551.

Engels, E. A., Atkinson, J. O., Graubard, B. I., Mcquillan, G. M., Gamache, C., Mbisa, G., Cohn, S., Whitby, D., and Goedert, J. J. (2007). Risk factors for human herpesvirus 8 infection among adults in the United States and evidence for sexual transmission. *J. Infect. Dis.* 196, 199–207.

Faris, M., Ensoli, B., Kokot, N., and Nel, A. E. (1998). Inflammatory cytokines induce the expression of basic fibroblast growth factor (bFGF) isoforms required for the growth of Kaposi's sarcoma and endothelial cells through the activation of AP-1 response elements in the bFGF promoter. *AIDS* 12, 19–27.

Flore, O., Rafii, S., Ely, S., O'Leary, J. J., Hyjek, E. M., and Cesarman, E. (1998). Transformation of primary human endothelial cells by Kaposi's sarcoma-associated herpesvirus. *Nature* 394, 588–592.

Friborg, J. Jr., Kong, W., Hottiger, M. O., and Nabel, G. J. (1999). p53 inhibition by the LANA protein of KSHV protects against cell death. *Nature* 402, 889–894.

Fujimuro, M., Wu, F. Y., Aprhys, C., Kajumbula, H., Young, D. B., Hayward, G. S., and Hayward, S. D. (2003). A novel viral mechanism for dysregulation of beta-catenin in Kaposi's sarcoma-associated herpesvirus latency. *Nat. Med.* 9, 300–306.

Ganem, D. (2005). *Kaposi's Sarcoma-Associated Herpesvirus.* Philadelphia: Lippincott Williams & Wilkins.

Gao, S. J., Boshoff, C., Jayachandra, S., Weiss, R. A., Chang, Y., and Moore, P. S. (1997). KSHV ORF K9 (vIRF) is an oncogene which inhibits the interferon signaling pathway. *Oncogene* 15, 1979–1985.

Gao, S. J., Deng, J. H., and Zhou, F. C. (2003). Productive lytic replication of a recombinant Kaposi's sarcoma-associated herpesvirus in efficient primary infection of primary human endothelial cells. *J. Virol.* 77, 9738–9749.

Grulich, A. E., Cunningham, P., Munier, M. L., Prestage, G., Amin, J., Ringland, C., Whitby, D., Kippax, S., Kaldor, J. M., and Rawlinson, W. (2005). Sexual behaviour and human herpesvirus 8 infection in homosexual men in Australia. *Sex. Health* 2, 13–18.

Hayward, G. S., and Zong, J. C. (2007). Modern evolutionary history of the human KSHV genome. *Curr. Top. Microbiol. Immunol.* 312, 1–42.

Hladik, W., Dollard, S. C., Mermin, J., Fowlkes, A. L., Downing, R., Amin, M. M., Banage, F., Nzaro, E., Kataaha, P., Dondero, T. J., Pellett, P. E., and Lackritz, E. M. (2006). Transmission of human herpesvirus 8 by blood transfusion. *N. Engl. J. Med.* 355, 1331–1338.

Hong, Y. K., Foreman, K., Shin, J. W., Hirakawa, S., Curry, C. L., Sage, D. R., Libermann, T., Dezube, B. J., Fingeroth, J. D., and Detmar, M. (2004). Lymphatic reprogramming of blood vascular endothelium by Kaposi sarcoma-associated herpesvirus. *Nat. Genet.* 36, 683–685.

Ishido, S., Wang, C., Lee, B. S., Cohen, G. B., and Jung, J. U. (2000). Downregulation of major histocompatibility complex class I molecules by Kaposi's sarcoma-associated herpesvirus K3 and K5 proteins. *J. Virol.* 74, 5300–5309.

Jenner, R. G., Maillard, K., Cattini, N., Weiss, R. A., Boshoff, C., Wooster, R., and Kellam, P. (2003). Kaposi's sarcoma-associated herpesvirus-infected primary effusion lymphoma has a plasma cell gene expression profile. *Proc. Natl. Acad. Sci. U.S.A.* 100, 10399–10404.

Kanno, T., Sato, Y., Nakamura, T., Sakamoto, K., Sata, T., and Katano, H. (2010). Genotypic and clinicopathological characterization of Kaposi's sarcoma-associated herpesvirus infection in Japan. *J. Med. Virol.* 82, 400–406.

Katano, H., Hoshino, Y., Morishita, Y., Nakamura, T., Satoh, H., Iwamoto, A., Herndier, B., and Mori, S. (1999a). Establishing and characterizing a CD30-positive cell line harboring HHV-8 from a primary effusion lymphoma. *J. Med. Virol.* 58, 394–401.

Katano, H., Sato, Y., Kurata, T., Mori, S., and Sata, T. (1999b). High expression of HHV-8-encoded ORF73 protein in spindle-shaped cells of Kaposi's sarcoma. *Am. J. Pathol.* 155, 47–52.

Katano, H., Iwasaki, T., Baba, N., Terai, M., Mori, S., Iwamoto, A., Kurata, T., and Sata, T. (2000a). Identification of antigenic proteins encoded by human herpesvirus 8 and seroprevalence in the general population and among patients with and without Kaposi's sarcoma. *J. Virol.* 74, 3478–3485.

Katano, H., Sato, Y., Kurata, T., Mori, S., and Sata, T. (2000b). Expression and localization of human herpesvirus 8-encoded proteins in primary effusion lymphoma, Kaposi's sarcoma, and multicentric Castleman's disease. *Virology* 269, 335–344.

Kazanji, M., Dussart, P., Duprez, R., Tortevoye, P., Pouliquen, J. F., Vandekerkhove, J., Couppie, P., Morvan, J., Talarmin, A., and Gessain, A. (2005). Serological and molecular evidence that human herpesvirus 8 is endemic among Amerindians in French Guiana. *J. Infect. Dis.* 192, 1525–1529.

Kedes, D. H., Ganem, D., Ameli, N., Bacchetti, P., and Greenblatt, R. (1997). The prevalence of serum antibody to human herpesvirus 8 (Kaposi sarcoma-associated herpesvirus) among HIV-seropositive and high-risk HIV-seronegative women. *JAMA* 277, 478–481.

Kellam, P., Bourboulia, D., Dupin, N., Shotton, C., Fisher, C., Talbot, S., Boshoff, C., and Weiss, R. A. (1999). Characterization of monoclonal antibodies raised against the latent nuclear antigen of human herpesvirus 8. *J. Virol.* 73, 5149–5155.

Lee, H., Veazey, R., Williams, K., Li, M., Guo, J., Neipel, F., Fleckenstein, B., Lackner, A., Desrosiers, R. C., and Jung, J. U. (1998). Deregulation of cell growth by the K1 gene of Kaposi's sarcoma-associated herpesvirus. *Nat. Med.* 4, 435–440.

Lei, X., Bai, Z., Ye, F., Xie, J., Kim, C. G., Huang, Y., and Gao, S. J. (2010). Regulation of NF-kappaB inhibitor IkappaBalpha and viral replication by a KSHV microRNA. *Nat. Cell Biol.* 12, 193–199.

Liao, W., Tang, Y., Lin, S. F., Kung, H. J., and Giam, C. Z. (2003). K-bZIP of Kaposi's sarcoma-associated herpesvirus/human herpesvirus 8 (KSHV/HHV-8) binds KSHV/HHV-8 Rta and represses Rta-mediated transactivation. *J. Virol.* 77, 3809–3815.

Liu, Z. Y., Ganju, R. K., Wang, J. F., Ona, M. A., Hatch, W. C., Zheng, T., Avraham, S., Gill, P., and Groopman, J. E. (1997). Cytokine signaling through the novel tyrosine kinase RAFTK in Kaposi's sarcoma cells. *J. Clin. Invest.* 99, 1798–1804.